Biogeotechnics 4 (2026) 100178

Contents lists available at ScienceDirect

Biogeotechnics

journal homepage: www.keaipublishing.com/en/journals/biogeotechnics/

Review Article

Bio-derived hierarchical micro/nanostructures from wood for energy conversion and storage

Jing Chen[a], Zidong Zhou[a], Yukun Bao[b], Abdul Mateen[a], Wei Yan[a], Jiawen Li[a], Yinfei Shao[a], Xiang Chen[a], Ghulam Farid[c], Zhihao Bao[a,*]

[a] School of Physics Science and Engineering, Tongji University, Shanghai 200092, China
[b] School of Electronic and Optical Engineering, Nanjing University of Science and Technology, Nanjing 210094, China
[c] Department of Applied Physics, University of Barcelona, C/Martí i Franquès, 1, Barcelona, Catalunya 08028, Spain

ARTICLE INFO

Keywords:
Wood
Lithium-sulfur batteries
Metal-oxygen batteries
Hierarchical porous structures

ABSTRACT

With the advancement of technology, the demand for environmentally friendly energy sources is increasing. Currently, the most commercially successful lithium-ion batteries cannot meet future demands due to their relatively low theoretical energy density. In contrast, lithium-sulfur batteries and metal-air batteries possess exceptionally high theoretical energy densities, making them the most promising candidates for next-generation batteries. However, several challenges remain before these batteries can be commercially viable on a large scale. Wood-derived materials, being abundant, environmentally friendly, biodegradable, and possessing unique hierarchical porous structures and excellent mechanical properties, present a remarkable potential for use in binder-free self-supporting electrodes and thick electrodes. These attributes offer a promising solution to the challenges faced by lithium-sulfur and metal-air batteries. This review highlights the application of wood-derived materials in next-generation high-performance batteries, specifically lithium-sulfur and metal-air batteries. It discusses the role of the hierarchical porous structures of wood-derived materials and outlines the challenges associated with their use. Additionally, it provides insights and ideas for future research directions in this area.

1. Introduction

With industrial development and social progress, the growing demand for energy has become a major challenge for humanity. Fossil fuels are non-renewable and cause serious environmental problems. Clean and renewable energy sources like wind and solar power, although promising, are intermittent and time-dependent, and their high development costs hinder large-scale utilization. Therefore, the advancement of electrochemical energy storage and conversion technologies will play a crucial role in addressing this issue. Lithium-ion batteries (LIBs), known for their high energy density, safety, and long cycle life, have been widely applied in mobile electronic devices and battery electric vehicles (Armand & Tarascon, 2008; Bruce et al., 2008; Goodenough & Park, 2013). However, the energy density of commercial lithium-ion batteries is approaching its upper limit, coupled with high costs, which fall short of meeting market demands. Therefore, the development of new rechargeable battery technologies is urgent, necessitating higher energy and power densities than LIBs, adequate safety measures, long cycle life, and relatively low costs. Metal-sulfur and metal-air batteries hold the highest theoretical energy densities and thus exhibit the greatest potential. Metal-sulfur and metal-air batteries boast extremely high theoretical energy densities, making them highly promising. However, metal-sulfur batteries still face challenges, including poor rate performance, low Coulombic efficiency, and significant capacity decay (Li et al., 2023; Tao et al., 2017; Wang, 2022a; Wen et al., 2023). Meanwhile, the performance of metal-air batteries is constrained by sluggish cathode kinetics. These factors prevent their widespread application. The key to overcoming these challenges lies in advancements in electrode materials. Based on the mechanisms of metal-sulfur and metal-air batteries, ideal cathode materials require excellent conductivity, hierarchically porous structures to facilitate the transport of electrolyte ions, and high-performance catalysts to enhance sluggish kinetic processes (Bruce, 2011b; Bruce et al., 2011a; Liu et al., 2017, 2019). Carbon materials possess excellent conductivity, high specific surface area, and are easily controllable in structure, making them widely applied in electrochemical energy storage and conversion devices (Liu et al., 2018, 2019; Yang et al., 2023). However, functionalized carbon materials with unique structures such as graphene and

* Corresponding author.
E-mail address: zbao@tongji.edu.cn (Z. Bao).

https://doi.org/10.1016/j.bgtech.2025.100178
Received 25 November 2024; Received in revised form 27 January 2025; Accepted 18 March 2025
Available online 7 July 2025

carbon nanotubes (CNTs) suffer from complex production processes and high costs, thereby limiting their applications (Jiang et al., 2016; Kim et al., 2015; Nomura et al., 2017). Biomass, with its wide availability, low cost, and eco-friendliness, has become an ideal source of carbon materials. Particularly, carbon materials derived from natural wood possess a unique layered porous structure (vertical channels and numerous micro/nano pores), excellent conductivity, and maintain good mechanical strength. This makes them well-suited as binder-free, self-supporting electrodes and carriers for thick electrodes in metal-sulfur and metal-air batteries (MABs) (Jiang et al., 2019; Schneidermann et al., 2019; Zhu et al., 2016). Wood-derived carbon materials were first reported as early as the 1990s (Byrne & Nagle, 1997). In 2004, they were initially used in LIBs, and it wasn't until 2015 and 2017 that wood-derived carbon materials were first applied in lithium-sulfur batteries (LSBs) and lithium-oxygen batteries (LOBs) (Adam et al., 2015; Luo et al., 2017; Wu et al., 2004). In recent years, numerous researchers have explored various strategies, including activation modification, surface modification, and composite with other metallic materials, to utilize wood-derived carbon materials in various battery components, such as anode, cathode, current collectors, and separators (Chen et al., 2021; Jiang et al., 2019; Song et al., 2019; Zhang, 2023a).

In recent years, several reviews have summarized the latest advancements of wood-derived carbon materials in electrochemical energy storage devices (Chen & Hu, 2021; Huang et al., 2019; Shan et al., 2021; Xu et al., 2022). However, these reviews often provide a broad overview of their application in metal-sulfur and metal-air batteries, without emphasizing the role of wood-derived materials' inherent layered porous structures. Therefore, this paper aims to discuss the role of wood-derived materials' hierarchically porous structures in metal-sulfur and metal-air batteries, along with the existing challenges.

Wood-derived materials, especially their porous biomass structure, have found widespread applications in fields such as batteries and electrochemical energy storage. At the same time, the use of wood and its derived materials in geotechnical engineering has gradually become a research hotspot. Geotechnical engineering, a vital branch of civil engineering, primarily involves foundation treatment, soil improvement, waste management, and groundwater management. In recent years, with increasing environmental concerns, traditional geotechnical engineering techniques have faced issues such as high resource consumption and significant environmental pollution, highlighting the urgent need for sustainable alternatives (Dong et al., 2024; Lv et al., 2022; Marathe & Sadowski, 2024; Wang, 2022b). Wood and bio-based geotechnical technologies, with their environmentally friendly, sustainable, and low-cost characteristics, provide new approaches and methods for geotechnical engineering.

2. The structure of wood

2.1. The structure of natural wood

Wood is a natural composite material composed of cellulose, hemicellulose, and lignin, featuring a hierarchical structure that spans multiple scales from meters to nanometers (Chen et al., 2020a). It ranges from meter-scale trunks to millimeter-scale wood tissues, and from micron-scale cells to nanometer-scale cellulose microcrystals. Basic nanoscale fibrils compose larger cellulose bundles on the order of tens of nanometers, which, together with hemicellulose and lignin, form the micrometer-scale cell walls. These cells are arranged in various ways to form different millimeter-scale wood tissues. Wood also exhibits pronounced anisotropic structures, particularly with numerous vertically aligned channels along the growth direction, serving as pathways for water, ions, and nutrient transport. The microstructure of wood has two essential requirements: first, it must ensure the efficient transport of water; second, it must provide adequate mechanical strength to support the upright growth of the tree. Generally speaking, larger pore sizes facilitate the transport of water and nutrients, while smaller, densely packed cell walls provide superior mechanical strength. These structural features are the result of "natural selection," typically determined by the species of the tree and its growing environment (such as temperature or rainfall). Based on differences in their microstructure, wood can be classified into hardwood and softwood. Softwood, typically derived from coniferous trees (e.g., pine, cedar, and spruce), has a simple and uniform structure, often consisting of vertically aligned, similarly shaped square channels. This allows for rapid growth, but results in a loosely packed, porous structure. Hardwood, generally comes from deciduous trees (e.g., balsa, lime, oak, birch, and poplar) and has a more complex structure. It typically consists of alternating larger and smaller diameter channels, where the larger channels facilitate the transport of water and nutrients to the trunk, while the smaller channels provide greater mechanical strength. This results in a dense yet porous structure for hardwood. In general, self-supporting electrodes in batteries require a hierarchical porous structure and sufficient mechanical strength. Therefore, hardwoods, with their more complex microstructure and superior mechanical properties, make more ideal precursors (Chen, 2020a; Chen & Hu, 2021; Shan et al., 2021; Wang, 2023a; Yu et al., 2019; Zhu et al., 2016).

2.2. Structure design of carbonized wood

Natural wood often undergoes carbonization and activation processes to acquire conductivity and develop a layered porous structure suitable for use in electrochemical energy storage devices.

Direct Carbonization Methods involve high-temperature pyrolysis of biomass materials under anaerobic or oxygen-deficient conditions to produce carbon materials with a certain degree of porosity (Liu et al., 2022; Tang et al., 2023). During pyrolysis, organic components undergo dehydration and decomposition, releasing gases that create pores in the material. For instance, Zheng et al. (2019) directly pyrolyzed poplar wood at different temperatures in an argon atmosphere to produce a series of hard carbon materials for sodium-ion battery anodes. The rich porous structure resulting from direct carbonization facilitated the transport of electrolyte ions, enabling the hard carbon material to exhibit a specific capacity of 330 mAh/g and an initial Coulombic efficiency of 88.3%. Similarly, Chen et al. (2017) achieved high conductivity, lightweight, and low bending carbon frameworks by directly carbonizing natural wood, which served as ultra-thick three-dimensional current collectors. Due to the unique biological structure, a three-dimensional conductive carbon framework with a thickness of 800 μm could accommodate 60 mg /cm^2 of lithium iron phosphate, providing a high discharge capacity of 7.6 mAh/cm^2 (95 Ah/L based on volume).

Hydrothermal Carbonization Methods involve that wood materials are placed in a reactor where water serves as the medium. Under anaerobic conditions and with heating and pressure, organic substances in biomass decompose to form carbon materials (Chen, 2022a; Li et al., 2024; Ming et al., 2013). The reaction temperature for hydrothermal carbonization typically ranges from 150 to 250 °C, with a reaction pressure of 2–10 MPa and a residence time of approximately 4–24 hours. During this process, the organic matter in biomass is converted into hydrothermal carbon mainly through processes such as dehydration, decarboxylation, polymerization, and dehydrogenation (Jain et al., 2016). For example, in the hydrothermal carbonization of cellulose, the cellulose chains undergo hydrolysis, producing various oligosaccharides (cellobiose, cellotetraose, cellotriose, and glucose). These oligosaccharides undergo a series of complex reactions, such as polymerization, intermolecular dehydration, or intramolecular dehydration, leading to an increase in molecular unsaturation and the formation of hydrothermal carbon. Detailed information can be found in the work of Sevilla & Fuertes (2009). The hydrothermal carbonization of biomass, such as starch, sucrose, cellulose, and hemicellulose, follows a similar process to that of cellulose. However, lignin in biomass is more resistant to hydrothermal reactions due to its compact structure, and it only undergoes hydrothermal reactions at temperatures above

200 ˚C. Kang et al. (2012) inferred that dissolved lignin exposed to water is decomposed to form phenolic resin, which then undergoes a series of complex reactions to generate hydrothermal carbon (Lou & Wu, 2011). For example, Li et al. (2024) employed a hydrothermal-assisted carbonization process to convert switchgrass into hard carbon anodes capable of efficiently storing sodium ions. The hydrothermal pretreatment effectively removed hemicellulose and impurities, creating a thermally stable precursor for hard carbon. These improvements resulted in enhanced initial Coulombic efficiency and cycling stability. The optimized hard carbon demonstrated a reversible specific capacity of 313.4 mAh/g at 100 mA /g, an initial Coulombic efficiency of 84.8%, and good cycling stability, with a capacity retention of 308.4 mAh/g after 100 cycles. Chen et al. (2020a) used graphite carbon nitride (g-C_3N_4) as a template to prepare nitrogen-doped porous carbonized wood fibers (N-PCF) through an in situ sacrificial template-assisted hydrothermal strategy. The hydrothermal process helped increase the specific surface area of the wood fibers, providing favorable conditions for subsequent doping. The results showed that N-PCF exhibited a large specific surface area, appropriate doping of heteroatoms, and abundant structural defects, leading to excellent electrochemical performance. The material demonstrated high specific capacities, delivering 434 mAh/g at 200 mA /g after 300 cycles in lithium-ion batteries and 266 mAh/g at 200 mA /g after 300 cycles in sodium-ion batteries.

Activation refers to the reaction between biomass feedstocks or precursors and activating agents, which causes some carbon atoms to be volatilized or gasified, resulting in the formation of numerous pores. The original pores further expand, and may even merge between pores, leading to a more complex pore structure. Common activators include oxidative gases (such as carbon dioxide and water vapor), zinc chloride ($ZnCl_2$), potassium hydroxide (KOH), and phosphoric acid (H_3PO_4). At high temperatures (typically 700 ℃ to 1000 ℃), CO_2 and water vapor oxidize carbon ($CO_2 + C \rightarrow 2CO$, $H_2O + C \rightarrow H_2 + CO$), causing them to vaporize and creating a porous structure. The advantages of this process are low production cost, environmental friendliness, and simplicity in operation. However, the activation process is difficult to adjust precisely, and the resulting porous structure is relatively disordered. For chemical activators, the reaction mechanisms differ. For example, phosphoric acid or potassium hydroxide, on one hand, depolymerize cellulose, hemicellulose, and lignin at lower temperatures, and through dehydration and condensation reactions, form H_2O. Water vapor at high temperatures vaporizes carbon atoms. On the other hand, they react with carbon to form polyphosphate groups, phosphates, K_2CO_3, etc., which causes some carbon to vaporize and creates a porous structure. Zinc chloride ($ZnCl_2$), on the other hand, volatilizes at high temperatures, forming a large number of mesopores and micropores (Cuña et al., 2014; Guo et al., 2024; Phiri et al., 2019; Zeng et al., 2024a). For example, Feng et al. utilized potassium carbonate and potassium hydroxide as activating agents to prepare activated carbon from wheat straw (Feng et al., 2021). They successfully adjusted the oxygen functional groups and pore volume of the activated carbon, achieving excellent oxygen reduction reaction (ORR) performance (half-wave potential of 0.77 V). This resulted in zinc-air batteries with high trip efficiency (60.7%) and long cycling life (280 hours/1680 cycles). Additionally, there have been reports on using CO_2 activation of various orientations of natural wood to obtain highly efficient supercapacitor electrodes (Cuña et al., 2014).

It's worth noting that traditional activation processes generate a significant amount of harmful substances, which is particularly concerning in the current context of increasing environmental issues (Wang, 2022c; Wu et al., 2023). Consequently, using biological enzymes or microorganisms to treat biomass materials offers an eco-friendly and pollution-free alternative with considerable potential. For instance, Wang et al (2022c). reported a method using fungal pretreatment of basswood to obtain hard carbon anodes for sodium-ion batteries. The experimental results demonstrated that the hard carbon anodes treated with fungi exhibited higher specific capacity (242.3 mAh/g at 200 mA /g), higher initial Coulombic efficiency (88.2%), and better cycling stability (93.9% capacity retention after 200 cycles). The differences in pore structures generated by various activation methods (such as the ratio of micropores, mesopores, and macropores) directly impact the cycling stability of the electrode. For example, a microporous structure can provide a larger surface area and more active sites, thereby increasing the initial capacity. However, an excess of micropores may lead to volume expansion of the hard carbon, causing structural degradation over prolonged charge-discharge cycles, which in turn affects the cycling stability.

Although biomass-derived carbon materials can generate a rich pore structure during the activation process, excessively large pores may lead to structural instability and make it difficult to maintain effective contact with the electrolyte, while excessively small pores can restrict the rapid diffusion of ions, thereby reducing the charge-discharge rate of the battery. Therefore, by precisely controlling factors such as the type and concentration of the activating agent, reaction temperature, and reaction time, the pore structure can be regulated to achieve optimal performance (Table 1).

2.3. Modification of carbonized wood structure

Although wood-derived carbon materials possess abundant pore structures, they primarily consist of vertical channels ranging from 30 to 200 μm and nanoscale pores on the pore walls for gas exchange. While excessively small pores can hinder the efficiency of electrolyte ion transport, overly large pores can reduce volumetric energy density and active material storage. Therefore, modifying the structure of carbonized wood can significantly enhance spatial utilization, increase active sites, and improve electrochemical performance (Huang et al., 2021; Wu et al., 2019, 2021). For example, Wu et al. (2021) introduced

Table 1
A summary of the preparation conditions and electrochemical performance of wood-derived materials.

Wood species	Carbonization condition	Activation condition	Applications	Electrochemical performance	Cycling stability	Ref.
Rosewood	1500 ℃ for 2 h	-	Sodium-ion batteries	430 mAh/g at 20 mA /g	280 mAh/g after 400 cycles at 500 mA /g	(Tang et al., 2023)
Eucalyptus wood	1400 ℃ for 2 h	-	Sodium-ion batteries	239 mAh/g at 100 mA/ g	293 mAh/g after 200 cycles at 100 mA/ g	(Liu et al., 2022)
Balsa wood	1400 ℃ for 2 h	-	Sodium-ion batteries	493 mAh/g at 100 mA/ g	248 mAh/g after 500 cycles at 100 mA/ g	(Jing et al., 2021)
Poplar wood	1400 ℃ for 2 h	-	Sodium-ion batteries	330 mAh/g at 5 C	94% after 600 cycles at 2 C	(Zheng et al., 2019)
Basswood	1300 ℃ for 6 h	Fungus-pretreated	Sodium-ion batteries	293 mAh/g at 100 mA/ g	243 mAh/g after 600 cycles at 200 mA/ g	(Wang et al., 2022c)
Willow wood	800 ℃ for 1 h	KOH	Supercapacitor	395 F/ g at 1 A /g in 6 mol/L KOH	94% after 5000 cycles at 5 C	(Phiri et al., 2019)
Fir wood	800 ℃ for 1.5 h	KOH	Supercapacitor	24.0 F /cm at 1 mA/ cm	98% after 10000 cycles at 100 mA/ cm^2	(Zeng et al., 2022b)
Makino wood	750 ℃ for 10 h	CO_2/H_2O	Supercapacitor	6.63 F/ cm at 1 mA/ cm	101.7 % after 10000 cycles	(Chen et al., 2022b)
Basswood	1000 ℃ for 3 h	-	Supercapacitor	3.04 F/ cm at 1 mA/ cm	82.2 % after 10000 cycles at 50 mA/ cm^2	(Wang et al., 2022d)

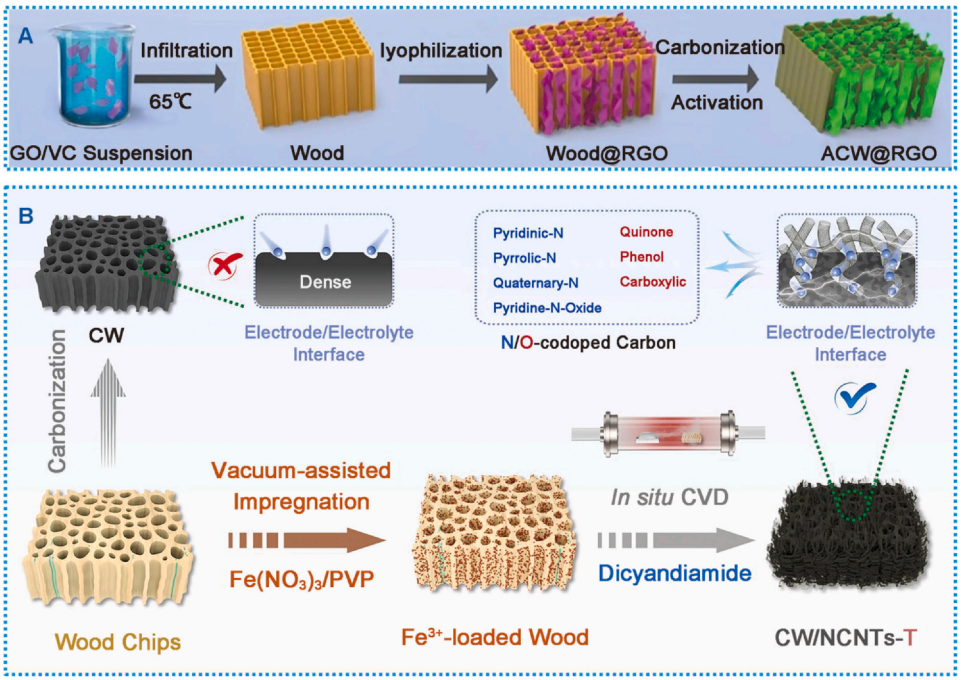

Fig. 1. (**A**) Schematic illustrating the fabrication of ACW@RGO hybrid (Wu et al., 2021); (**B**) Systematic illustration for the preparation of CW/NCNTs-T composite electrodes (Yan et al., 2024).

a GO/ascorbic acid suspension into wood, followed by freeze-drying, carbonization, and KOH activation to obtain ACW@RGO electrodes (Fig. 1A). The reduced graphene oxide (RGO) nanosheets interlinked within the wood's pore channels, forming a three-dimensional porous structure. Thanks to the secondary structure formation and KOH activation, ACW@RGO exhibited a high specific surface area of 1049.9 m^2/g and an excellent areal capacitance of 26.6 F/cm^2 at a current density of 1 mA/cm^2. Similarly, Yao et al. (2023) used a method involving MXene nanosheets to construct a secondary structure, resulting in CW/MXene electrodes. The CW/MXene electrode demonstrated a high capacitance of 14.48 F/cm^2 (203.94 F/g) at a current density of 1 mA/cm^2.

Unlike the top-down approach of filling materials into the wood's pore channels, Yan et al. (2024) employed a bottom-up method. They used Fe-based nanoparticles as a catalyst and dicyandiamide as a carbon source, growing N-doped CNTs in situ within CW through chemical vapor deposition (CVD) to obtain CW/NCNTs electrodes (Fig. 1B). Benefiting from the designed hierarchical porous structure and doped heteroatom functional groups, CW/NCNTs exhibited high initial specific capacitance (5762 mF/cm^2 in a three-electrode system and 4480 mF/cm^2 in a two-electrode system) and excellent long-term cycling stability (30,000 cycles in the three-electrode system and 20,000 cycles in the two-electrode system). Although growing secondary structures on wood-derived materials can achieve sufficiently high capacity and excellent cycling stability, further improvements in electrochemical performance can still be achieved through surface modification and doping, composite metal oxides, and optimization of pore structures. Additionally, optimizing the electrolyte formulation can ensure that these materials maintain good performance even in low-temperature environments (Luo et al., 2022; Xia et al., 2016; Yao et al., 2021; Zeng, 2022a).

3. Application of wood-derived materials in lithium-sulfur batteries

Lithium-sulfur batteries typically consist of a lithium metal anode, an organic electrolyte containing lithium ions, and a sulfur cathode. Each sulfur atom can bond with two lithium atoms (one S_8 molecule can bond with 16 Li atoms), giving lithium-sulfur batteries a higher theoretical specific capacity (1675 mAh/g) and theoretical energy density (2600 Wh /kg), which is 3–5 times higher than traditional lithium-ion batteries (Bruce et al., 2011a; Carbone et al., 2017; Kim et al., 2023a; Nguyen et al., 2023). The discharge process of the sulfur cathode primarily involves three steps: firstly, solid to solution reduction of S_8 molecule into long-chain polysulfides; secondly, solution phase reduction of long-chain polysulfides into short-chain polysulfides; finally, solution to solid reduction of the short-chain polysulfides into Li_2S_2 and Li_2S. Due to the insolubility and insulating nature of Li_2S_2 and Li_2S, discharge termination and reduced energy density are issues. Additionally, during charge and discharge cycles, the sulfur cathode undergoes significant volume changes (~80%), leading to electrode material pulverization and rapid capacity decay. Furthermore, the shuttle effect of polysulfides occurs, where soluble polysulfides (Li_2S_x, $4 \leq x \leq 8$) shuttle between the cathode and anode, reduce active material utilization and Coulombic efficiency. Moreover, lithium metal anodes tend to form dendrites during repeated charge-discharge cycles, posing safety challenges for LSBs (Chen et al., 2020b). Researchers have made significant improvements, such as composite cathodes, functional binders, surface-coated separators, and modified electrolytes, among others.

3.1. Wood-derived materials for cathodes of LSBs

Wood-derived materials feature a distinctive biological structure. Vertical channels aid in electrolyte transport, while abundant nanoscale pores enhance polysulfide adsorption, mitigating shuttle effects. Additionally, the three-dimensional porous structure of wood facilitates increased loading of active materials, enabling high sulfur loading in thick electrodes. For example, Ge et al. (2023) prepared wood-derived hierarchical porous carbon frameworks as three-dimensional conductive scaffolds for assembling high-performance LSBs (Fig. 2B). The micron-scale pores of wood facilitate electrolyte diffusion. Through CO_2 activation, a large number of nanoscale pores are introduced on the micron-scale tube walls, which can suppress the dissolution and shuttle effect of lithium polysulfides, thereby enhancing the battery's rate capability and cycling performance. This enables the S@WHCF cathode to achieve a specific capacity of 1120 mAh/g at a rate of 0.1 C, with

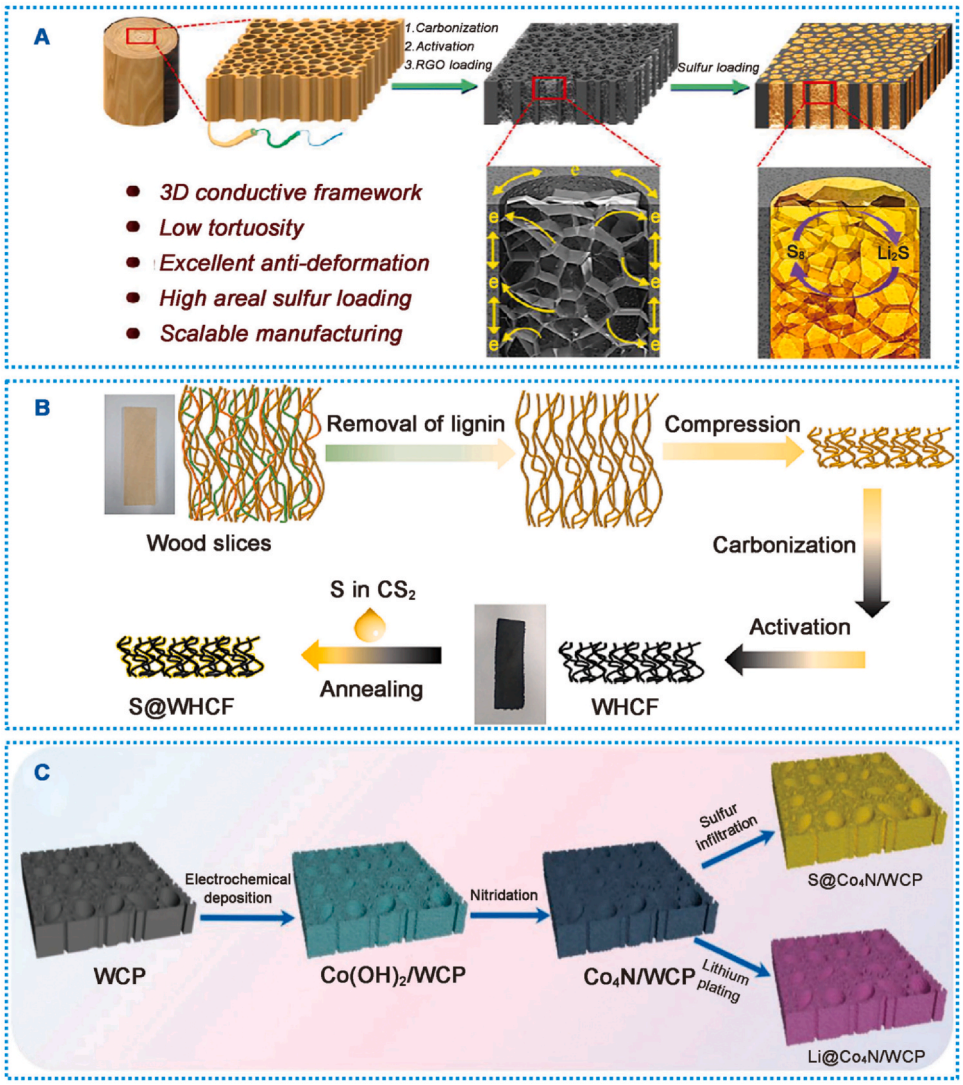

Fig. 2. (**A**) Schematic illustration of the preparation process and structure of the S@C-wood composite electrode (Li et al., 2017); (**B**) Schematic diagram of the preparation of wood-derived hierarchical porous carbon frameworks (Ge et al., 2023); (**C**) Schematic illustration of Co_4N/WCP host fabrication (Zhang et al., 2022a).

excellent cycling stability at high rates (0.5 C and 1 C). Adam et al. (2015) prepared a layered hierarchical carbon derived from natural wood, termed as biomorphic carbon derived carbon (CDC) material. They initially activated wood templates using steam or carbon dioxide and employed a precursor of poly-carbosilane and halogenation treatment to create a layered porous material. This material boasts a high specific surface area of up to 1750 m^2/g, a micro/mesopore volume of 1.0 cm^3/g, and a macropore volume of 1.2 cm^3/g. Its efficient mass transfer in the layered porous structure enables stable capacities exceeding 580 mA h/g at current densities exceeding 20 mA /cm^2 (2 C), with high sulfur utilization and extremely low electrolyte content of 6.8 μL /mg . Li et al. (2017) employed microchannel-filled reduced graphene oxide (RGO) to create a high-sulfur-loading three-dimensional porous scaffold (Fig. 2A). Thanks to its characteristics of low curvature, high conductivity, and excellent structural stability, the three-dimensional porous carbon matrix exhibits low curvature, high electrical conductivity, and good structural stability. Wood-based lithium-sulfur batteries achieve a high sulfur loading of 21.3 mg/ cm^2 and a high areal capacity of 15.2 mAh/cm^2. Sabet et al. (2023) utilized delignified and low-temperature pyrolysis methods to obtain delignified wood-derived carbon (CDW), which was then impregnated with sulfurized polyacrylonitrile (SPAN) for use as a cathode in lithium-sulfur batteries (SPAN@CDW). SPAN is a promising cathode active material capable of suppressing the dissolution of lithium polysulfides in Li-S batteries. However, due to the low sulfur content in SPAN, CDW enables high loading of SPAN. The unique three-dimensional conductive porous structure ensures efficient transport of electrons and ions. The SPAN@CDW electrode exhibits a discharge capacity of $>$ 1000 mAh/g at 1 C (1672 mA/ g) and maintains a high specific capacity of ~1350 mA h/g after 500 cycles at 0.1 C. Zhang et al. (2022a) designed wood-derived carbon plates decorated with Co_4N nanoparticles (Co_4N/WCP), serving as carriers for sulfur cathodes and lithium metal anodes (Fig. 2C). The Co_4N/WCP electrode significantly enhances the reaction kinetics of sulfur cathodes and promotes uniform lithium plating on lithium metal anodes. This enables full cells using S@Co_4N/WCP as the cathode and Li@Co_4N/WCP as the anode to exhibit excellent cycling stability with a high areal sulfur loading of 4 mg/ cm^2. After 500 cycles at 1 C rate, the cells deliver a specific capacity of 807.9 mAh/g.

3.2. Wood-derived materials for separators of LSBs

Due to the hierarchical porous structure of wood-derived materials, which includes numerous micropores and mesopores capable of adsorbing polysulfides and suppressing shuttle effects, they are often used in separators or interlayers for LSBs. For example, Chen et al. (2021)

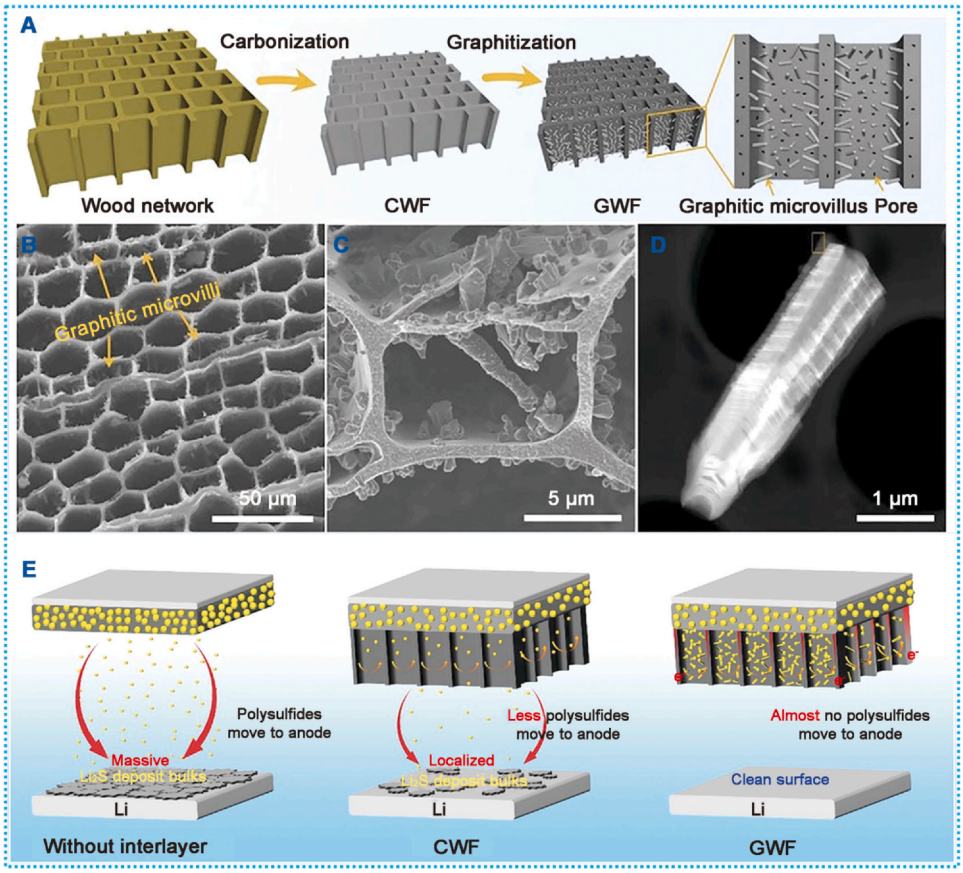

Fig. 3. (**A**) Schematic illustration of the preparation processes for GWF with the volume and structure changed; (**B**) Cross-sectional and (**C**) magnified scanning electron microscope (SEM) images of GWF showing abundant graphitic microvilli grown on the tunnel surfaces; (**D**) HAADF image of a graphitic microvillus; (**E**) Schematic illustration of different interlayers affecting the electrochemical performance of Li–S batteries. (A) – (E) are from Chen et al. (2021).

engineered a wood-derived highly graphitic framework (GWF) with a porous tunnel structure and microvelvet surface as an interlayer for LSBs (Fig. 3A – E). The GWF retains the three-dimensional transport network of wood while providing additional deposition sites for polysulfides via microvelvet growth on the inner surfaces of carbon tunnels. This design feature enables the GWF to achieve high initial discharge capacity (1593 mAh/g at 0.05 C) and excellent cycling performance (0.06% capacity decay per cycle at 1 C). Huang et al. (2023) utilized a straightforward hydrothermal method to in situ generate Mo_2S_3 with abundant sulfur vacancies on wood, further depositing graphene oxide (GO) to replace traditional polyolefin membranes as separators. Through theoretical calculations, simulations, and experiments, they demonstrated that GO@NWC/Mo_2S_3 separator materials not only promote the conversion of lithium polysulfides (LiPS) but also facilitate uniform lithium plating. In lithium symmetrical cells, GO@NWC/Mo_2S_3 exhibited an exceptionally long electroplating/stripping lifespan of up to 8000 hours at a low voltage of 0.1 V and maintained a specific capacity of 377 mAh/g after 2000 cycles at 1 C current density, with a capacity decay rate of 0.036% per cycle, demonstrating outstanding cycling stability.

4. Application of wood-derived materials in metal-air batteries

A typical metal-air batteries consists of a metal anode, an air cathode, and an electrolyte containing metal salts. Known metal anodes include Li, Na, Zn, Mg, Al, and Fe, with the active material for the cathode primarily sourced from oxygen in the air (Ye et al., 2020; Julien, 2023; Chen et al., 2020c). During the discharge and charge cycles of MABs, the anode undergoes metal stripping and deposition processes, while the cathode undergoes the oxygen reduction reaction and the oxygen evolution reaction (OER). Depending on the type of electrolyte used—aqueous or non-aqueous—the anode/cathode reactions vary. Aqueous electrolytes are used with less active metal anodes such as Zn, Al, Mg, and Fe, as the low cost of water helps reduce material costs. Non-aqueous electrolytes, on the other hand, protect active metals like lithium and sodium from corrosion by water and moisture. Due to the semi-open structure of MABs, which use oxygen from the air as the active material without occupying the mass of the electrode material itself, they possess extremely high energy density, making them one of the most promising next-generation batteries (Li et al., 2016; Lu et al., 2014; Yuan, 2023a). However, the issues of metal anode corrosion, passivation, and dendrite growth, along with the sluggish reaction kinetics at the air cathode, have hindered the commercialization of MABs.

Wood-derived materials, as a sustainable and environmentally friendly resource, have gained widespread attention in battery technology in recent years, particularly in improving the performance of metal-air batteries (MABs). Wood-derived materials possess a high specific surface area and porous structure. The high specific surface area allows for the loading of a large number of reactive sites, while the porous structure accommodates reaction products and facilitates material transport, both of which contribute to enhancing the electrochemical performance of MABs. On the other hand, wood-derived materials exhibit excellent conductivity, mechanical strength, and chemical stability, providing unmatched advantages for use in self-supporting thick batteries, leading to higher gravimetric and volumetric energy densities. Additionally, due to their unique structure and mechanical strength, wood-derived materials can serve as the framework for lithium metal anodes or solid-state electrolytes, enabling MABs to maintain long-term stability (Jin et al., 2018; Song et al., 2019; Yang et al., 2022).

4.1. Lithium-oxygen batteries

Due to lithium's lowest electronegativity, atomic number, and density among all metals, lithium-oxygen batteries have the highest energy density of all metal-air batteries, reaching up to 3500 Wh/ kg (based on Li_2O_2) (Wang, 2023a; Wong et al., 2024). This is nearly nine times that of traditional LIBs (387 Wh/ kg). In aprotic LOBs, during the discharge process, oxygen reacts with Li^+ to form solid Li_2O_2 ($2Li^+ + O_2 + 2e^- \leftrightarrow Li_2O_2$, $E^0 = 2.96V$). The cathode reaction in LOBs involves solid, liquid, and gas phase changes. During the ORR, lithium metal at the anode is oxidized to Li^+ ions, which migrate through the organic electrolyte to the positive electrode, while electrons travel through an external circuit to the positive electrode. At the cathode, O_2 is reduced by the catalyst on the electrode surface into superoxide anion (O^{2-}) and peroxide anion (O_2^{2-}), which combine with Li^+ from the electrolyte to form the insoluble discharge product lithium peroxide (Li_2O_2), depositing on the positive electrode surface. The OER involves the decomposition of Li_2O_2 into lithium ions and oxygen gas during the charging process. Li^+ migrate back through the organic electrolyte to the anode, where they gain electrons and are reduced to lithium metal, while O_2 gas is released into the environment. Since the discharge product Li_2O_2 is insoluble in the organic electrolyte and is an insulator, it accumulates during discharge, blocking ion and gas transport channels and covering the catalyst surface, which increases charge transfer resistance and eventually halts the discharge process (Johnson et al., 2014; Tan et al., 2022; Yao et al., 2019). Moreover, due to the difficulty in decomposing Li_2O_2, higher potentials are often required for its decomposition. This results in higher charging voltages, which can lead to the decomposition of the electrolyte and carbon materials. Consequently, this decomposition causes a rapid decline in capacity during cycling. Furthermore, the Li metal anode faces challenges such as corrosion, passivation, and the formation of lithium dendrites. These issues significantly hinder the large-scale application of LOBs (Ma et al., 2018; Shu, 2019).

To address these challenges, researchers have made substantial efforts, including designing high-performance composite cathodes, protecting lithium metal anodes, developing solid-state electrolytes, and exploring redox mediators. Wood-derived materials, with their hierarchical porous structure, vertically aligned channels, and micropores, facilitate the transport of Li^+ and O_2. Moreover, their abundant nanoscale pores enable the loading of numerous active sites and storage of discharge products, making them ideal candidates as cathode materials for LOBs. Currently, dual-function catalysts used in LOBs mainly include carbon-based catalysts, noble metal catalysts, and transition metal-based catalysts.

Carbon materials are often chosen for electrode materials due to their low cost, excellent conductivity, and controllable structure. However, pure carbon materials typically exhibit insufficient OER activity, leading to significantly elevated charging potentials. Element doping induces charge redistribution, enhances adsorption of intermediate species, facilitates charge transfer, activates catalytic sites, and thereby improves the catalytic performance of LOBs (Kopiec et al., 2024; Yang et al., 2023; Yu, 2023a). For example, Luo et al. (2017) utilized NH_3 thermal treatment of natural pine wood to successfully prepare N-doped carbonized wood electrode (wd-NC). Thanks to nitrogen doping, wd-NC exhibited a discharge capacity of approximately 1.86 mAh/cm^2 at a current density of 0.08 mA/ cm^2, which is about five times higher than that of pure carbonized wood electrode wd-C (0.38 mAh/cm^2).

Noble metal catalysts, such as Pt, Pd, and Ru, exhibit significantly higher catalytic performance than carbon materials and are commonly used in LOBs (Dai et al., 2021; Jung et al., 2021; Xing et al., 2020). For example, Song et al. (2017) designed a "breathable" carbonized wood electrode by depositing ruthenium nanoparticles as catalysts within the carbonized wood (Fig. 4A and B). The Ru nanoparticles were uniformly distributed on the walls of the aligned channels, providing numerous reaction sites. Additionally, the porous channel walls soaked with electrolyte formed a continuous thin electrolyte layer, facilitating rapid Li^+ transport. Consequently, this material achieved a high specific areal capacity of 8.58 mAh/cm^2 at a current density of 0.1 mA/ cm^2 with an electrode thickness of approximately 700 μm. Similarly, Zhu et al. (2018) utilized RuO_2 nanoparticles loaded within the pores of carbonized wood as the cathode for LOBs. Benefiting from the microchannel structure that enhances oxygen and lithium ion transport, and the numerous active sites generated by CO_2 activation, the RuO_2/WD-C cathode achieved a specific areal capacity exceeding 8 mAh/cm^2 at 0.1 mA/ cm^2 with a charging voltage below 3.8 V. Notably, this material could be reused after deep charge-discharge cycles through a simple water wash. However, while carbonized wood electrodes possess good conductivity, they lack flexibility, limiting their application in flexible electronic devices. To address this, Chen et al. (2019) reported a wood-derived electrode for flexible LOBs (Fig. 4C−E). They transformed rigid and electrically insulating natural balsa wood into flexible and conductive material through delignification and subsequent coating with CNTs and Ru nanoparticles. The resulting cell walls, composed of cellulose nanofibers with abundant nanopores, facilitated Li^+ transport, while vertically aligned microchannels served as pathways for O_2 transport. The CNT film coating the microchannels acted as an electronic transport channel. This unique non-competitive three-channel design enabled the wood-based cathode to exhibit a low overpotential of 0.85 V at 100 mA /g, a record high areal capacity of 67.2 mAh/cm^2, and a long cycle life of 220 cycles.

Although noble metal catalysts possess excellent catalytic performance, their high cost limits large-scale application. Consequently, researchers have turned their attention to more affordable transition metal-based catalysts. Common transition metal-based catalysts include transition metals and their compounds, such as oxides, nitrides, carbides, phosphides, and sulfides. For instance, Jing et al. (2022) developed a Co and N co-doped wood-derived electrode using a molten salt method (Fig. 5A). During the carbonization process, high-energy ions etched the carbon framework, creating a porous structure while successfully incorporating Co and N elements into the carbon matrix, with Co primarily existing as single atoms or atomic clusters. Consequently, this material exhibited high specific capacity (a discharge specific capacity of 9.44 mAh/cm^2 at a current density of 0.05 mA/ cm^2) and good cycling stability (113 cycles at a limited capacity of 0.5 mAh/cm^2). Similarly, Zhao et al. (2019) used Co-MOF as a precursor to uniformly distribute mesoporous Co_3O_4/C polyhedrons on the CW tube walls for LOBs (Fig. 5B). The rapid material transport and uniform reaction interface enabled the Wood-D/Co_3O_4/C electrode to demonstrate excellent reversibility and cycling stability (over 380 cycles at a current density of 1.0 mA/ cm^2 with a capacity limit of 1.0 mAh/ cm^2). Liang et al. (2023) developed an Fe_3C-decorated N-doped wood-derived electrode (N-wdC-MS) through a one-step pyrolysis of Paulownia wood and melamine, impregnated with $FeCl_3$/LiCl (Fig. 5C). The etching effect of the $FeCl_3$/LiCl mixed molten salt enlarged the pore structure of the carbonized wood, expanding the three-phase boundary, while Fe_3C@NC aggregates grew uniformly on the channel surfaces of the carbonized wood. As a result, LOBs assembled with N-wdC-MS as the cathode delivered a high discharge capacity of 50.28 mAh/cm^2 and a cycling life of 190 cycles at a current density of 0.1 mA/ cm^2.

The semi-open system of LOBs can lead to electrolyte depletion, lithium anode corrosion, and byproduct deposition, thereby limiting their practical application. However, the unique biological structure of wood offers remarkable potential in addressing these challenges. For example, Zhang et al. (2023a) designed a novel natural wood separator through delignification and one-step thermal treatment for use in LOBs (Fig. 6A−D). This separator utilizes capillary action to retain the electrolyte, and after 40 days in an open environment, it maintained 39% of its initial electrolyte absorption capacity, significantly higher than glass fiber (GF, 15%). Additionally, the wood-derived separator exhibited higher ionic conductivity (5.11 mS/cm) and a lithium-ion transference number of 0.74, which inhibited deposition on the wood channels and corrosion of the lithium anode. This resulted in excellent anode reversibility (over 1200 hours) and cathode longevity (over 300 cycles).

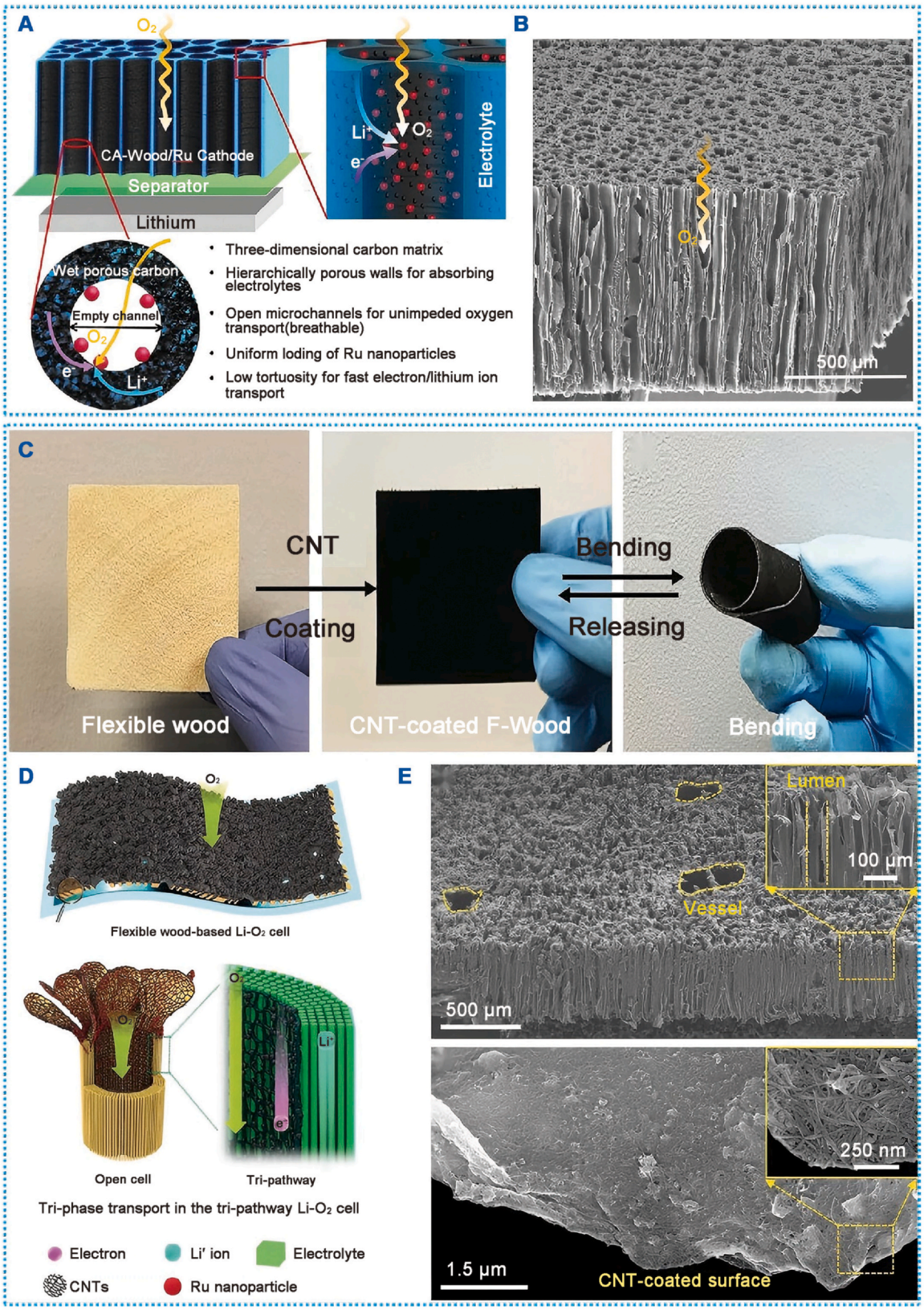

Fig. 4. (**A**) Schematic diagram of the Li-O_2 batteries with the CA-wood/Ru cathode; (**B**) SEM images of CA-wood/Ru cathode; (**A**) and (**B**) are from Song et al. (2017); (**C**) Photographs of the original F-Wood, CNT-coated F-Wood, and bent CNT-coated F-Wood membranes; (**D**) A tri-pathway structural design; (**E**) SEM images of the CNT-coated F-Wood membrane; (A) – (C) are from Chen et al. (2019).

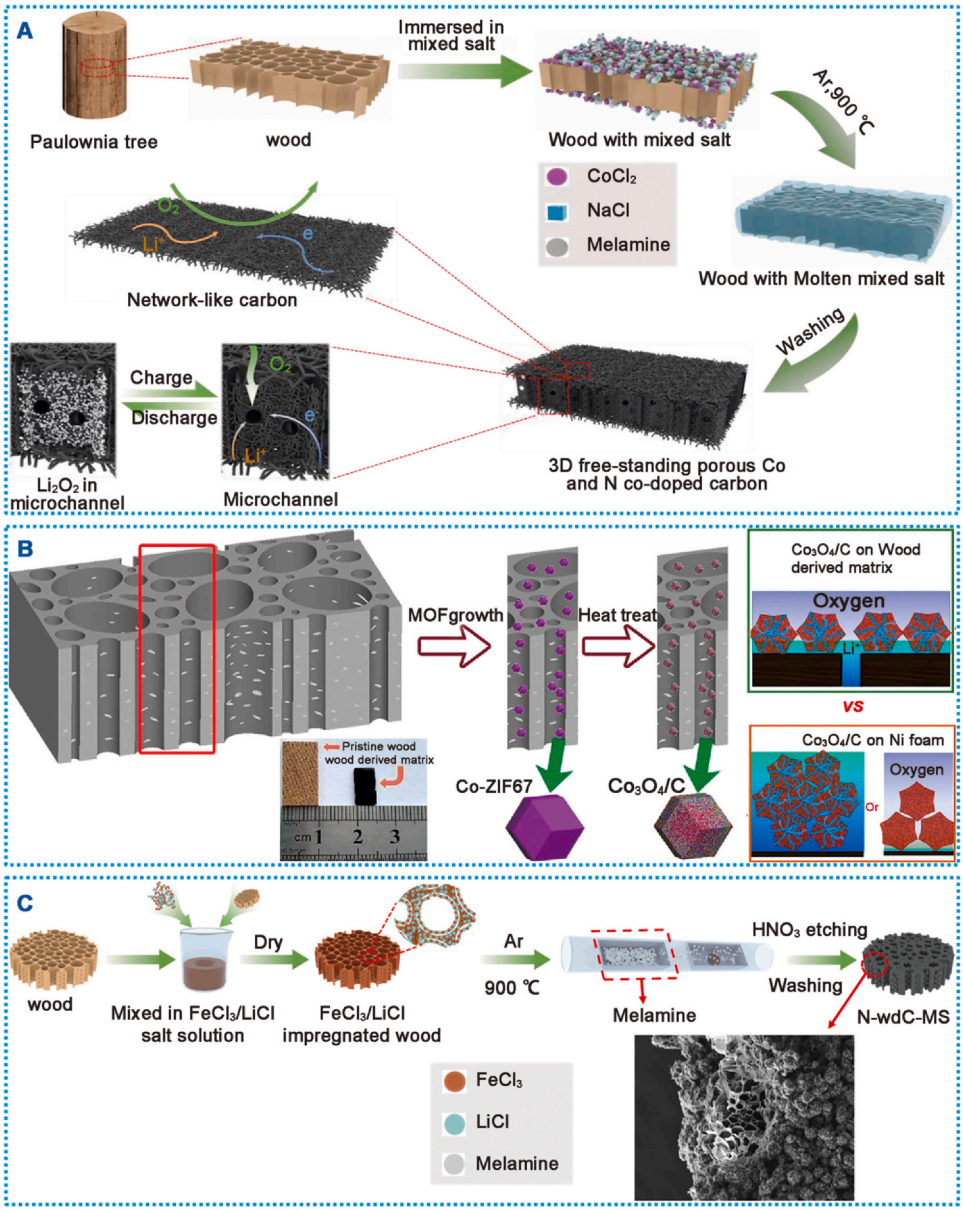

Fig. 5. (**A**) The synthesis strategy of Nx-wdC-900 cathode (Jing et al., 2022); (**B**) Schematic diagram of the preparation of Co_3O_4/C modified Wood-D substrates (Zhao et al., 2019); (**C**) Schematic diagram for the preparation of N-wdC-MS (Liang et al., 2023).

4.2. Zinc-air batteries

Zinc-air batteries (ZABs) are similar to LOBs, but they use a zinc metal anode and aqueous electrolytes. Compared to LOBs, ZABs offer a high energy density (approximately 1086 Wh /kg), which is slightly lower than LOBs. However, due to the abundance of zinc in the Earth's crust (approximately 300 times more than lithium) and the use of cheaper aqueous electrolytes, ZABs present a significant cost advantage (Cui, 2017; Gao et al., 2023; Lv et al., 2024; Song et al., 2020). Additionally, zinc metal is stable in air and aqueous electrolytes, providing enhanced safety. These factors make primary ZABs the only commercially successful metal-air batteries to date. Nevertheless, there are still challenges in commercializing rechargeable ZABs. The electrode reactions in rechargeable ZABs typically occur in alkaline solutions. During discharge, the zinc metal anode is oxidized to form $Zn(OH)_4^{2-}$, which spontaneously decomposes into zinc oxide (ZnO). Concurrently, the oxygen reduction reaction (ORR) occurs at the cathode, reducing oxygen to OH^-. The charging process reverses these reactions: ZnO reacts with H_2O and OH^- to regenerate $Zn(OH)_4^{2-}$, which is then reduced to Zn at the anode, while the oxygen evolution reaction (OER) occurs at the cathode, oxidizing OH^- to oxygen (Lv et al., 2024). The overall electrode reactions can be described as follows:

$$2Zn + O_2 \leftrightarrow 2ZnO(1.65Vvs.\ SHE)$$

Currently, the performance of rechargeable ZABs is limited by the catalytic activity of the cathode catalysts and the corrosion and dendrite formation on the zinc metal anode. Natural wood-derived materials, with their hierarchical porous structure, can ensure the rapid transport of electrolytes and oxygen while hosting numerous catalytic/deposition sites, making them ideal candidates for both cathode and anode substrates in ZABs.

Carbonized wood exhibits good electrical conductivity, robust mechanical properties, and a layered porous structure. However, pure carbon materials typically lack ORR/OER activity, rendering carbonized wood unsuitable for direct use as a self-supporting cathode in ZABs. Doping with heteroatoms can alter the electronic structure, enhancing the adsorption of intermediates and promoting charge transfer, which facilitates ORR/OER reactions (Deng et al., 2023; Peng et al.,

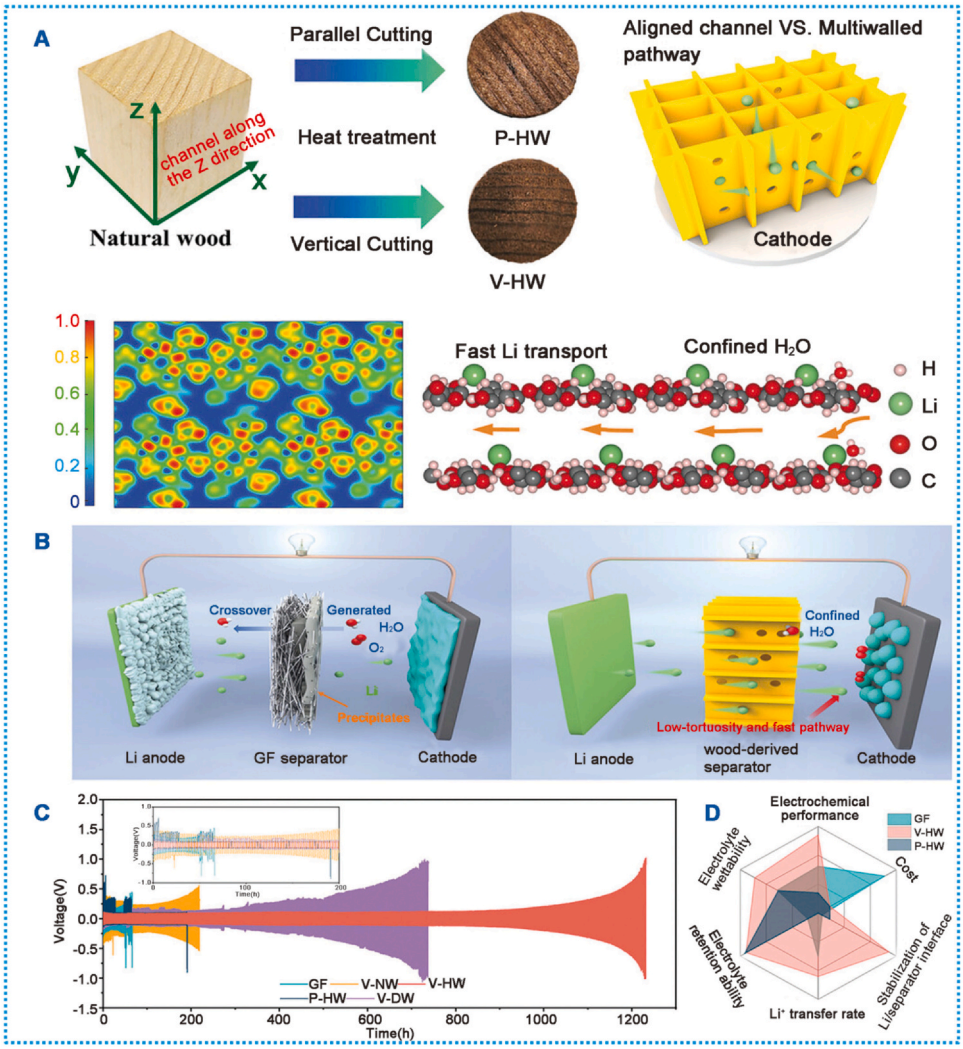

Fig. 6. (**A**) Graphical illustration of wood with multiple aligned channels under different cut directions and preparing conditions, where the lithium-ions could migrate along the oriented cellulose in the wood fiber. Electron localization function (ELF) maps show a uniform electron distribution. (**B**) Schematic of operation principle for wood-derived separator in LOBs; (**C**) Cyclic performance of symmetric Li/separator/Li cells at a current density of 1.0 mA/ cm^2 and 1.0 mAh/cm^2; (**D**) Comparison of the general properties of the separators. (**A**) – (**D**) are from Zhang et al. (2023a).

2019). For instance, Deng et al. (2023) prepared a three-dimensional nitrogen-doped carbon self-supporting electrode (TNCSE) by thermally treating and acid-activating raw wood materials (Fig. 7A – C). The activation process successfully doped nitrogen atoms, creating more active sites and significantly boosting electrochemical activity. Crucially, the porous microchannels in the carbon framework of TNCSE not only allow for rapid Zn^{2+} transport but also form three-phase reaction interfaces on the porous walls of the microchannels, resulting in excellent battery performance. This enabled a ZAB with a TNCSE cathode to achieve a peak power density of 134.02 mW/ cm^2 and continuous charge-discharge for 500 hours. Similarly, Peng et al. (2019) used cellulase treatment on natural wood, followed by a subsequent thermal treatment to dope nitrogen into the carbon framework (Fig. 7D – H). By soaking the wood overnight in an aqueous solution containing cellulase, the cellulase selectively hydrolyzes the cellulose into soluble monosaccharides, resulting in the formation of numerous shallow nanopores on its surface. The enzyme effectively hydrolyzed part of the cellulose in the natural wood, creating numerous nanopores. Carbonization then formed a three-dimensional porous conductive network, maximizing the exposure of active sites. Consequently, when used in ZABs, this material achieved a specific capacity of 801 mAh/g, an energy density of 955 Wh/ kg, and long-term stability of up to 110 hours.

To further enhance the performance of ZABs, metal materials are often loaded onto carbon substrates to achieve stronger catalytic activity. However, the high cost of precious metals limits their widespread application. Consequently, designing cost-effective transition metal-based ORR/OER catalysts is crucial for improving performance of ZABs. Transition metal-based catalysts primarily include transition metals and alloys, as well as transition metal compounds such as oxides, hydroxides, nitrides, phosphides, sulfides, and carbides (Liu, et al., 2020, 2023; Poudel et al., 2024; Wang, 2022e; Yan et al., 2021).

Wang et al. (2023b) synthesized nitrogen-doped wood-derived carbon supported $FeNi_3$ alloy for a self-supported electrode with dual-function catalytic activity ($FeNi_3$@NWC). $FeNi_3$ alloy nanoparticles coupled with nitrogen-doped carbon expedite the catalytic activity toward ORR by promoting proton generation on $FeNi_3$ and transfer to nitrogen-doped carbon. The potential gap of only 0.68 V between ORR and OER of $FeNi_3$@NWC is achieved. The liquid zinc-air batteries (ZABs) with $FeNi_3$@NWC convey a robust lifetime of ~266 h (800 cycles) with stable charging and discharging. Zhang et al. (2023a) loaded Mn-doped Co nanoparticles on nitrogen-doped cedar-derived carbon as a dual-function catalyst (CoMn-N@NCW). Due to electronic interactions between the bimetallic components and rapid mass transport in porous carbon, CoMn-N@NCW exhibited excellent ORR/OER

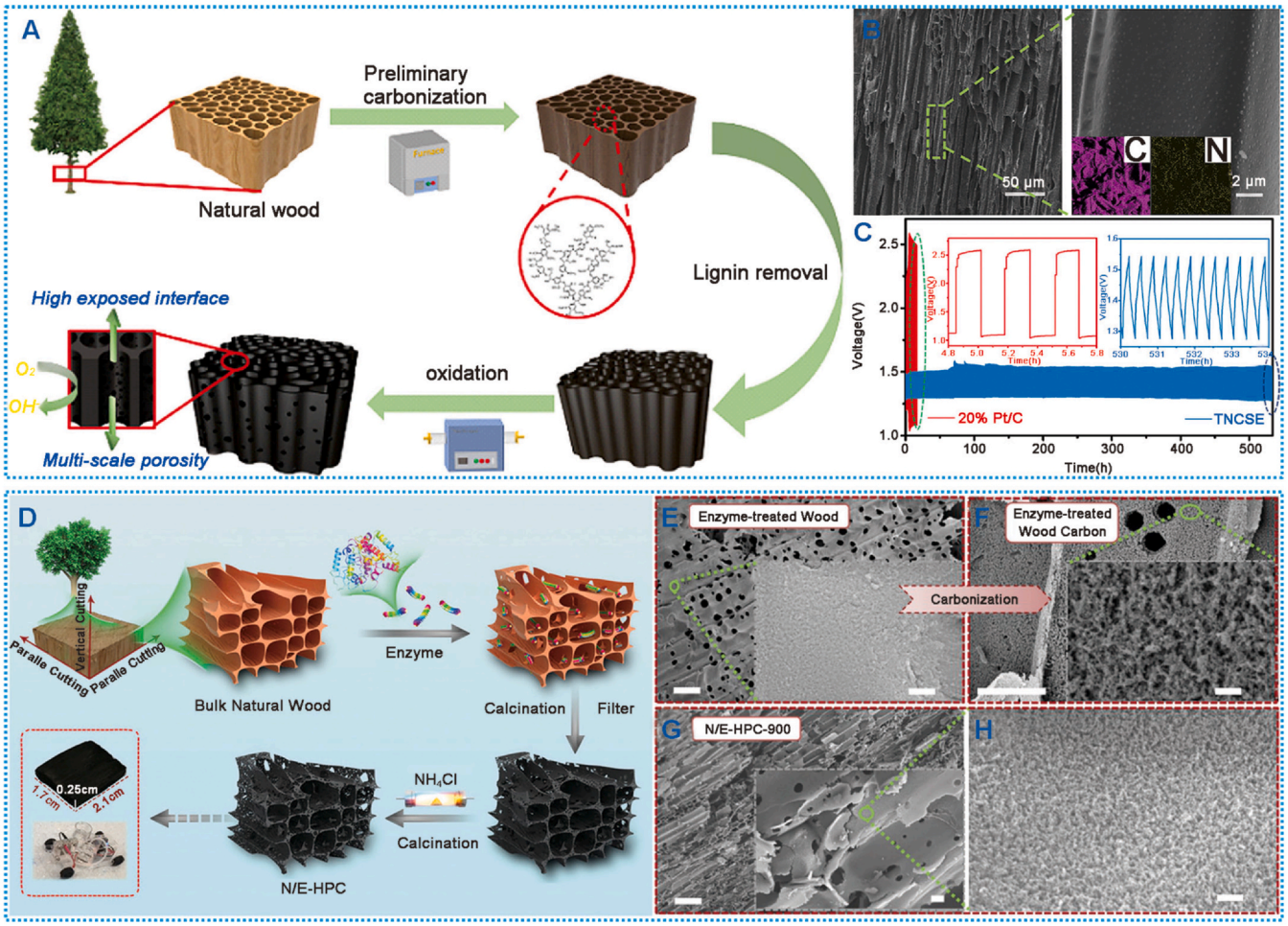

Fig. 7. (**A**) Schematic diagram of the synthesis of TNCSE; (**B**) SEM image of TNCSE; (**C**) Charge/discharge stability test curves of ZAB assembled with TNCSE and 20% Pt/C; (A) – (C) are from Deng et al. (2023). (**D**) Schematic of bulk transformation process using the enzyme-assisted method. (E) – (H) SEM images of enzyme-treated wood plate, enzyme-treated wood plate after carbonization, and N/E-HPC-900 sample obtained by pyrolysis of enzyme-treated wood carbon with NH_4Cl in N_2 with different magnifications. (D) – (H) are from Peng et al. (2019).

activities (ΔE of 0.68 V). Liquid-state ZABs assembled with CoMn-N@NCW achieved an open circuit voltage of 1.542 V, peak power density of 186 mW/ cm^2, and long-term cycling stability of 600 hours. Moreover, quasi-solid-state ZABs using CoMn-N@NCW showed an open circuit voltage of 1.493 V and 70 hours of cycling stability. Pang et al. (2021) utilized a convenient delignification method to convert natural balsa wood into layered porous carbon material (Fig. 8F – G). FeCo alloy supported by N and S-doped wood-based carbon aerogels (FeCo@NS-CA) was employed as the cathode for rechargeable flow ZABs. The resulting layered porous structure facilitated rapid substance transport and exposed numerous active sites, leading to outstanding ORR/OER activities. For ORR, FeCo@NS-CA exhibited an onset potential of 0.97 V and a half-wave potential of 0.85 V, comparable to commercial Pt/C electrodes. For OER, FeCo@NS-CA achieved an overpotential of 450 mV, similar to benchmark RuO_2. ZABs assembled with FeCo@NS-CA operated at a current density of 10 mA/ cm^2, achieving a power density of 140 mW/ cm^2 and a specific capacity of 760 mA h/g, demonstrating greater stability (400 hours) compared to ZABs using Pt/C and RuO_2 cathodes.

Zhang et al. (2023b) assembled nitrogen-doped cedar wood (CW) with two-dimensional nickel-iron hydroxide nanosheets (NiFe-LDH@NC). The unique interface structure between biochar and NiFe-LDH accelerated electron transfer during oxygen electrocatalysis, imparting durability to NiFe-LDH@NC for both ORR and OER processes. Similarly, Zhou et al. (2024) fabricated an independent self-supported carbon composite electrode (CoNiLDH@NPC) composed of nitrogen and phosphorus co-doped cedar wood (NPC) and CoNi layered double hydroxides (CoNiLDH). Due to its large specific surface area and unique defect structure, CoNiLDH@NPC exhibited strong interface folding effects in the two-dimensional to three-dimensional nanostructure, demonstrating outstanding dual-function catalytic activity. Moreover, the highly ordered open channels in wood provided ample space, forming abundant three-phase boundaries to accelerate catalytic processes. As a result, zinc-air batteries using CoNiLDH@NPC showed high power densities (aqueous: 263 mW/ cm^2, quasi-solid-state: 65.8 mW/ cm^2) and long-term stability (aqueous: 500 hours, quasi-solid-state: 120 hours).

Zhou et al. (2024) successfully fabricated a dual-metal cobalt-iron alloy/oxide decorated wood-derived carbon electrode (CoFe-$CoFe_2O_4$@WDC). Benefitting from its layered porous structure that provides excellent three-phase interfaces for multiphase reactions, CoFe-$CoFe_2O_4$ formed rich heterogeneous structure interfaces that facilitated electron transfer. Under alkaline conditions, the optimized composite electrode exhibited a significantly high half-wave potential of 0.85 V and exceptionally low overpotential of 1.49 V. It also demonstrated stable performance over 2340 cycles in applications of ZABs. Meanwhile, Cui et al. (2021) prepared nitrogen-doped wood-derived carbon electrodes decorated with Co/CoO via electrochemical deposition and thermal treatment (Co/CoO@NWC) (Fig. 8A – E). ZABs assembled with Co/CoO@NWC cathodes showed high discharge specific capacity (800 mAh/g), low charge-discharge gap (0.84 V), and long-term cycling stability (270 hours) in liquid-state configurations. Moreover, they exhibited significant catalytic activity and stability in full solid-state ZAB configurations as well.

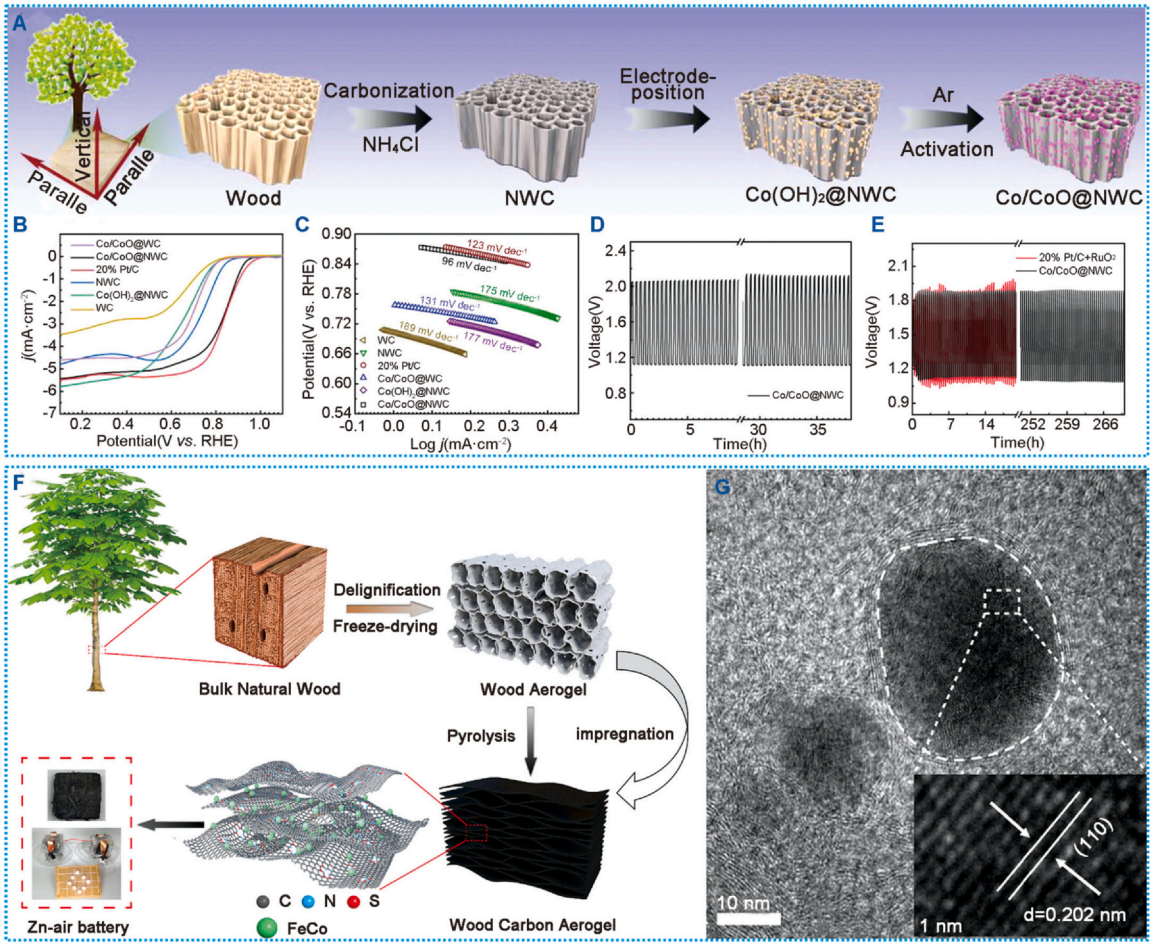

Fig. 8. (**A**) Schematic illustration for the construction of integral Co/CoO@NWC electrode; (**B**) Linear sweep voltammetry (LSV) curves for oxygen reduction reaction (ORR) on WC, NWC, Co/CoO@WC, $Co(OH)_2$@NWC, Co/CoO@NWC and 20% Pt/C at 1600 r/min; (**C**) Tafel plots for ORR on WC, NWC, Co/CoO@WC, Co(OH)2@NWC, Co/CoO@NWC and 20% Pt/C; (**D**) Galvanostatic discharge curves of all-solid-state ZAB at 2 mA/ cm^2; (**E**) Galvanostatic discharge/charge cycling curves of rechargeable ZABs (the ZABs were constructed with Co/CoO@NWC-powder or 20% Pt/C + RuO_2 as catalysts for the air electrode); (A) – (E) are from Cui et al. (2021). (**F**) Schematic diagram of the synthesis process of FeCo@NS-CA; (**G**) HRTEM image of one FeCo nanoparticle. (F) and (G) are from Pang et al. (2021).

Zhang et al. (2022b) successfully prepared nitrogen-doped wood-derived catalytic activated carbon decorated with FeP nanoparticles (NPs) (FeP-NWCC), achieving a dual-function catalytic electrode (FeP-NWCC) (Fig. 9A – D). In alkaline environments, FeP-NWCC exhibited excellent catalytic activity for both ORR ($E_{1/2}$ = 0.86 V) and OER (overpotential of 310 mV at 10 mA/ cm^2). Liquid-state ZABs assembled with FeP-NWCC showed outstanding peak power density (144 mW/ cm^2) and cycling stability (over 450 hours). Quasi-solid-state ZABs based on FeP-NWCC also demonstrated excellent performance. Zhang et al. (2024b) also synthesized cobalt-doped FeP decorated nitrogen-doped wood-derived carbon electrodes (CoFeP@NBC). By doping Co into FeP, the D-band center of Fe in CoFeP@NBC was adjusted, enhancing its ORR/OER activities. CoFeP@NBC exhibited an ORR $E_{1/2}$ of 0.88 V and an OER overpotential of 300 mV at 10 mA/ cm^2, with ΔE of 0.65 V. In liquid-state ZABs, CoFeP@NBC maintained high stability with negligible charge-discharge voltage hysteresis (0.01 V) after over 2400 cycles (800 hours). Quasi-solid-state ZABs assembled with CoFeP@NBC also demonstrated considerable performance.

Li et al. (2021) synthesized dual-active site catalysts combining Fe_3C nanoparticles with nitrogen-doped paulownia wood-derived carbon (Fe_3C@NPW). One active site, the Fe_3C nanoparticles, facilitated water molecule activation, while the nitrogen-doped carbon at another site activated oxygen molecules. Benefitting from the synergistic effect of dual-active sites, Fe_3C@NPW exhibited significant catalytic activity for ORR with a half-wave potential of 0.87 V (vs RHE). Zinc-air batteries (ZABs) assembled with Fe_3C@NPW as the cathode catalyst achieved a high specific capacity of 804.4 mAh/ g and maintained long-term stability over 780 cycles. Solid-state ZABs based on this model also demonstrated satisfactory performance with an open circuit voltage of 1.39 V and a peak power density of 78 mW/ cm^2.

Single-atom catalysts (SACs) are attractive due to their high electrocatalytic activity, excellent durability, and 100% utilization of active atoms (Yuan et al., 2023b). Wood, with its unique layered porous structure, serves as an ideal carrier for SACs and a strong candidate for cathodes of ZABs. For instance, Zhou et al. (2021) synthesized a three-dimensional integrated air electrode containing Co-N sites and layered porous carbon (Co-N@ACS) through co-doping growth and simultaneous pyrolysis with ZIF-8. The layered porous structure promoted oxygen diffusion and electrolyte penetration, exposing numerous Co-N sites, thereby endowing Co-N@ACS with ultra-high ORR activity ($E_{1/2}$ = 0.86 V). Assembled in a liquid-state zinc-air battery, Co-N@ACS achieved an open circuit voltage of 1.46 V, peak power density of 155 mW/ cm^2, and long-term stability over 540 cycles (180 hours). In solid-state zinc-air batteries, Co-N@ACS exhibited a high open circuit voltage of 1.36 V and a low charge-discharge voltage gap (0.8 V). Zhong et al. (2021) employed a simple Lewis acid pre-treatment and carbonization process to in-situ generate single-atom Fe-N-C catalysts on wood-based porous carbon (Fig. 9E). The Lewis acid $FeCl_3$ pre-treatment not only generated abundant microchannels in the wood cell walls but also successfully dispersed atomic Fe-N active species into the hierarchical structure. These uniformly dispersed SACs on the layered structure enhanced the performance and durability of ORR/OER. ZABs

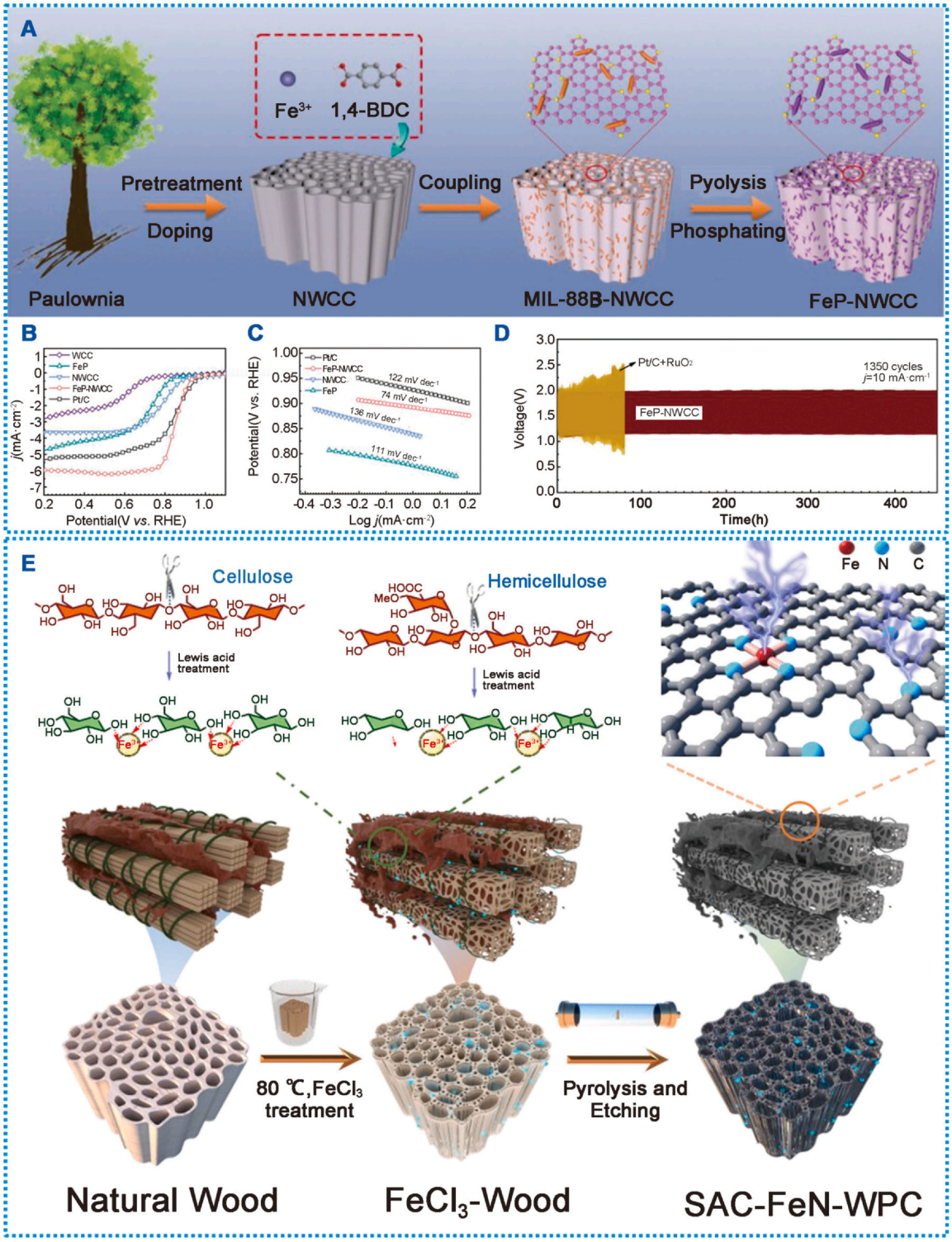

Fig. 9. (**A**) Scheme for the synthesis of FeP-NWCC; (**B**) LSV curves of WCC, NWCC, FeP, FeP-NWCC, Pt/C-20%; (**C**) Tafel plots of NWCC, FeP, FeP-NWCC, Pt/C-20%; (**D**) Cyclic charge–discharge test of ZABs FeP-NWCC and 20% Pt/C + RuO_2 at 10 mA/ cm^2. (A) – (D) are from Zhang et al. (2022b). (**E**) Schematic illustration of the fabrication procedure of SAC-FeN-WPC (Zhong et al., 2021).

using catalysts at the cathode demonstrated high power density (70.2 mW/ cm^2 in quasi-solid-state) and long-term stability.

4.3. Aluminum-air batteries

Similar to ZABs, aluminum-air batteries (AABs) utilize metallic aluminum as the anode, offering a theoretical specific energy density of up to 8135 Wh/ kg. The electrochemical reactions of aluminum-air batteries in alkaline aqueous electrolytes can be described as follows (Kim, 2023b; Wang et al., 2024; Yu, 2023b):

$$4Al + 3O_2 + 6H_2O \leftrightarrow 4Al(OH)_3 \quad (2.71Vvs.\ SHE)$$

Similarly, a major drawback of AABs is their low Coulombic efficiency, high polarization due to corrosion of the metallic anode, and

sluggish ORR kinetics. Researchers have addressed these issues through measures such as designing high-performance cathodes, protecting the anode, and developing novel structures for AABs. Yu et al. (2023b) demonstrated the feasibility of wood-based gas diffusion electrodes (GDEs) for aluminum-air batteries using cobalt-nitrogen co-doped carbon nanotubes as ORR catalysts (Fig. 10A and B). Benefiting from their hierarchical porous structure, the GDEs achieved higher power density compared to commercial carbon fiber paper electrodes (267 vs.

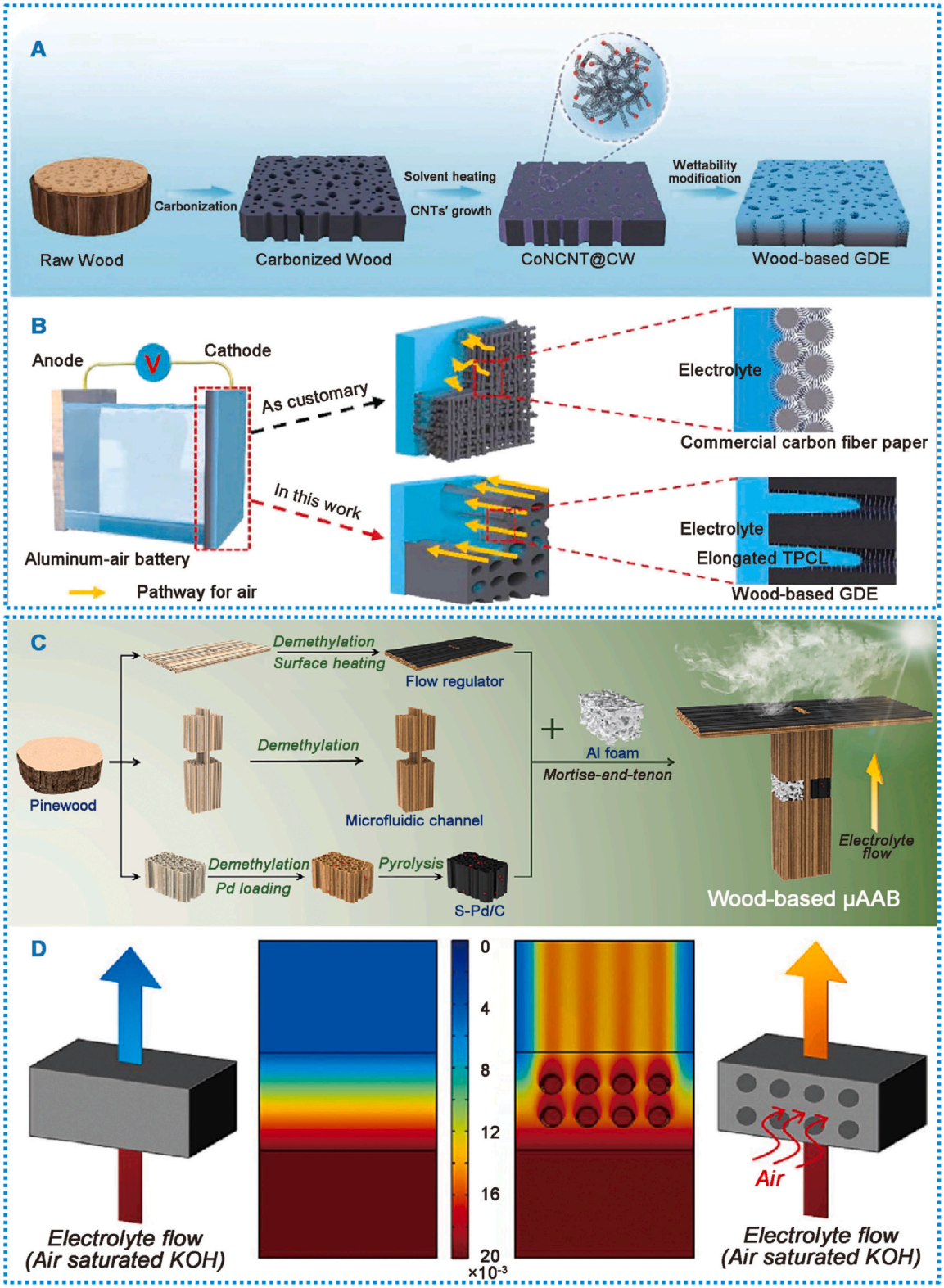

Fig. 10. (**A**) Schematic diagram of the fabrication process of cherry wood-based GDE; (**B**) Schematic diagram of the principle of vertical pore gradient wetting carbonized wood air electrode compared with conventional carbon paper air electrode; (A) and (B) are from Yu et al. (2023b). (**C**) Schematic illustration of the preparation process and the configuration of a wood-based μAAB coupled with a photothermal evaporation driven flow regulator; (**D**) Simulated O_2 concentration in the S-Pd/C cathode electrode with and without pore structure. (C) and (D) are from Wang et al. (2024).

236 mW/ cm^2). Wang et al. (2024) introduced a novel photothermal-driven microfluidic wood-based aluminum-air battery (μAABs) (Fig. 10C and D). Utilizing naturally aligned microchannels in wood for electrolyte transport, partially charred wood acted as a photothermal evaporator for flow regulation, and wood-derived freestanding carbon cathodes were employed for oxygen reduction reactions. These components were assembled using mortise and tenon joints, resulting in μAABs exhibiting a significant peak power density of 230 mW/ cm^3. The superior performance stems from enhanced mass transfer facilitated by the wood-derived cathode's three-dimensional channel structure, electrochemical interfaces, and minimized depletion boundary layers. Continuous electrolyte flow stability was achieved for over 11 hours (200 mA/ cm^3) through the photothermal evaporator in the μAABs, promoting stable operation.

5. Conclusion and prospects

Lithium-sulfur batteries and metal-air batteries possess exceptionally high theoretical energy densities, making them promising candidates for next-generation energy storage solutions. However, several challenges remain before they can achieve large-scale commercialization. Given the similarities between lithium-sulfur batteries and metal-air batteries—such as sluggish reaction kinetics, insoluble and non-conductive discharge products, and involvement in two-phase/three-phase reactions—both types of batteries require cathodes with similar characteristics. These include excellent conductivity, hierarchical porous structures, and superior catalytic performance.

In this review, we highlight the application of wood-derived materials in lithium-sulfur and metal-air batteries. Wood-derived materials exhibit unique bio-derived hierarchical porous structures, with microscale pores facilitating material transport, and nanoscale pores providing sites for active species and accommodating discharge products. Due to their excellent mechanical properties, wood-derived materials can serve as self-supporting thick electrodes without binders in lithium-sulfur and metal-air batteries. This eliminates the risk of pore blockage by binders and reduces unnecessary mass, thereby achieving high energy density. For these reasons, we consider natural wood to be a highly promising source of electrode materials.

Wood-derived materials have inherent advantages, such as sustainability and environmental friendliness, but in commercial applications, cost is often a limiting factor. While wood itself is a cheap raw material, the complex processing involved may lead to high costs. On one hand, large-scale production should be implemented to reduce costs; on the other hand, cheaper sources of wood, such as fast-growing or waste wood, should be selected. Additionally, more efficient and cost-effective chemical treatments, such as hydrothermal methods and CO_2 or H_2O activation, should be adopted. Wood-derived materials often demonstrate excellent battery performance at the laboratory scale, but scaling up to mass production presents numerous challenges, including consistency and quality control, and material processability. These issues can be addressed through the development of specialized equipment for processing wood-derived materials, the creation of new processing and treatment techniques, and ensuring the standardization of the manufacturing process.

Despite the progress made in applying wood-derived materials in lithium-sulfur and metal-air batteries, several challenges remain. Here, we outline some difficulties and propose potential solutions:

1) The large pores in wood can lead to wasted space, while excessively small pores can hinder material transport. Therefore, rational design of pore structures is essential. On one hand, multi-scale pore design should be conducted to find the optimal combination of micropores, mesopores, and macropores. For example, advanced computer simulations (such as molecular dynamics simulations or finite element simulations) can be used to predict the impact of pore structure on battery performance, and experimental data can be combined to optimize pore design. On the other hand, secondary structures can be built inside the wood channels (e.g., by utilizing carbon nanotubes or graphene to construct a three-dimensional structure) to achieve higher energy density.
2) The performance of lithium-sulfur and metal-air batteries based on wood-derived materials still needs improvement. Nanotechnology and interface engineering should be utilized to enhance battery performance. For example, nanotechnology can be used to enhance the conductivity and ionic conductivity of wood-derived materials. By coating the surface of these materials with conductive layers or conductive nanoparticles (such as carbon nanotubes, graphene, or metal nanoparticles), the interface stability between the material and the electrolyte can be improved, thereby reducing impedance and enhancing long-cycle stability. Alternatively, chemical modification or coating can optimize the electrochemical stability of wood-derived materials, improving their conductivity and reactive activity in batteries.
3) The metal anodes in lithium-sulfur and metal-air batteries are prone to corrosion, passivation, and dendrite formation. Further research is needed to develop wood-derived metal anodes and solid electrolytes. For example, thanks to the unique structure and excellent mechanical properties of wood-derived materials, they can serve as the framework for lithium metal anodes. On one hand, this enhances the mechanical performance of the lithium metal anode, and on the other hand, the rich pore structure of wood-derived materials provides numerous nucleation sites, which help lithium metal to be deposited and stripped uniformly during long charge-discharge cycles, achieving long-term cycle stability. Furthermore, the vertically aligned parallel channels and good mechanical strength of wood make it suitable as a supporting structure for solid-state electrolytes, reducing lithium anode dendrite formation and corrosion, thereby ensuring better cycling stability. Additionally, as a separator for MABs, wood-derived materials can effectively reduce electrolyte volatility, resulting in a longer cycle life.
4) To make wood-derived materials more practical, the design of high energy density battery structures based on wood is essential. On one hand, high energy density design should be pursued, using composite material design or constructing secondary structures, incorporating high energy density active materials into wood-derived materials to improve the battery's specific energy. On the other hand, computer simulations can be used to optimize the structural design of the battery, making it more efficient at accommodating active materials and maintaining stable electrochemical performance. Alternatively, the structural design can allow for self-supporting electrodes made from wood-derived materials to be easily disassembled and replaced, enabling regeneration or recycling.
5) To meet various demands, the mechanical properties of wood-derived materials, including mechanical strength and flexibility, should be enhanced. For example, by combining wood-derived materials with high-strength materials (such as carbon fiber or graphene) or through heat treatment, the mechanical strength of the wood-derived materials can be enhanced, ensuring the electrochemical performance while improving the mechanical stability of the battery structure. Alternatively, by using special treatment methods, conductive nanomaterials (such as carbon nanotubes or graphene) can be incorporated into wood-derived materials, making them flexible while also conductive, thus enabling their use in flexible conductive devices.

CRediT authorship contribution statement

Jing Chen: Writing – original draft, Visualization, Investigation, Formal analysis, Data curation, Conceptualization. **Zidong Zhou:** Investigation, Data curation. **Yukun Bao:** Investigation. **Abdul Mateen:** Investigation. **Wei Yan:** Investigation, Formal analysis. **Jiawen Li:** Investigation, Formal analysis. **Yinfei Shao:** Investigation,

Data curation. **Xiang Chen:** Visualization, Investigation. **Ghulam Farid:** Investigation. **Zhihao Bao:** Writing – review & editing, Supervision, Project administration, Funding acquisition, Formal analysis.

Declaration of Competing Interest

The authors declare that they have no known competing financial interests or personal relationships that could have appeared to influence the work reported in this paper.

Acknowledgements

It was funded by Shanghai Key Laboratory of Special Artificial Microstructure Materials and Technology.

References

Adam, M., Strubel, P., Borchardt, L., Althues, H., Dörfler, S., & Kaskel, S. (2015). Trimodal hierarchical carbide-derived carbon monoliths from steam- and CO_2-activated wood templates for high rate lithium sulfur batteries. *Journal of Materials Chemistry A, 3*(47), 24103–24111. https://doi.org/10.1039/c5ta06782k

Armand, M., & Tarascon, J. M. (2008). Building better batteries. *Nature, 451*(7179), 652–657. https://doi.org/10.1038/451652a

Bruce, P. G., Freunberger, S. A., Hardwick, L. J., & Tarascon, J. M. (2011b). Li–O_2 and Li–S batteries with high energy storage. *Nature materials, 11*(1), 19–29.

Bruce, P. G., Hardwick, L. J., & Abraham, K. M. (2011a). Lithium-air and lithium-sulfur batteries. *MRS Bulletin, 36*(7), 506–512.

Bruce, P. G., Scrosati, B., & Tarascon, J. M. (2008). Nanomaterials for rechargeable lithium batteries. *Angewandte Chemie International Edition in English, 47*(16), 2930–2946. https://doi.org/10.1002/anie.200702505

Byrne, C. E., & Nagle, D. C. (1997). Carbonized wood monoliths—characterization. *Carbon, 35*(2), 267–273. https://doi.org/10.1016/s0008-6223(96)00135-2

Carbone, L., Greenbaum, S. G., & Hassoun, J. (2017). Lithium sulfur and lithium oxygen batteries: New frontiers of sustainable energy storage. *Sustainable Energy Fuels, 1*(2), 228–247. https://doi.org/10.1039/c6se00124f.

Chen, C., Kuang, Y., Zhu, S., Burgert, I., Keplinger, T., Gong, A., ... Hu, L. (2020a). Structure–property–function relationships of natural and engineered wood. *Nature Reviews Materials, 5*(9), 642–666.

Chen, L., Yu, H., Li, W., Dirican, M., Liu, Y., & Zhang, X. (2020b). Interlayer design based on carbon materials for lithium–sulfur batteries: a review. *Journal of Materials Chemistry A, 8*(21), 10709–10735.

Chen, X., Ali, I., Song, L., Song, P., Zhang, Y., Maria, S., ... Ramakrishna, S. (2020c). A review on recent advancement of nano-structured-fiber-based metal-air batteries and future perspective. *Renewable and Sustainable Energy Reviews, 134*, 110085.

Chen, Y., Wu, Y., Liao, Y., Zhang, Z., Luo, S., Li, L., ... Qing, Y. (2022a). Tuning carbonized wood fiber via sacrificial template-assisted hydrothermal synthesis for high-performance lithium/sodium-ion batteries. *Journal of Power Sources, 546*, 231993.

Chen, Y., Yu, Y., Zhang, X., Guo, C., Chen, C., Wang, S., & Min, D. (2022b). High performance supercapacitors assembled with hierarchical porous carbonized wood electrode prepared through self-activation. *Industrial Crops and Products, 181*, 114802.

Chen, C., & Hu, L. (2021). Nanoscale ion regulation in wood-based structures and their device applications. *Advanced Materials, 33*(28), Article e2002890. https://doi.org/10.1002/adma.202002890

Chen, C., Xu, S., Kuang, Y., Gan, W., Song, J., Chen, G., ... Hu, L. (2019). Nature-inspired tri-pathway design enabling high-performance flexible Li–O_2 batteries. *Advanced Energy Materials, 9*(9), 1802964. https://doi.org/10.1002/aenm.201802964

Chen, C., Zhang, Y., Li, Y., Kuang, Y., Song, J., Luo, W., ... Hu, L. (2017). Highly conductive, lightweight, low-tortuosity carbon frameworks as ultrathick 3D current collectors. *Advanced Energy Materials, 7*(17), 1700595. https://doi.org/10.1002/aenm.201700595

Chen, Y., Zou, K., Dai, X., Bai, H., Zhang, S., Zhou, T., ... Guo, Z. (2021). Polysulfide filter and dendrite inhibitor: Highly graphitized wood framework inhibits polysulfide shuttle and lithium dendrites in Li–S batteries. *Advanced Functional Materials, 31*(31), 2102458. https://doi.org/10.1002/adfm.202102458

Cui, Z., Fu, G., Li, Y., & Goodenough, J. B. (2017). Ni_3FeN-supported Fe_3Pt intermetallic nanoalloy as a high-performance bifunctional catalyst for metal–air batteries. *Angewandte Chemie International Edition, 56*(33), 9901–9905.

Cui, X., Liu, Y., Han, G., Cao, M., Han, L., Zhou, B., & Jiang, J. (2021). Wood-derived integral air electrode for enhanced interfacial electrocatalysis in rechargeable Zinc-Air battery. *Small, 17*(38), Article 2101607. https://doi.org/10.1002/smll.202101607

Cuña, A., Tancredi, N., Bussi, J., Barranco, V., Centeno, T. A., Quevedo, A., & Rojo, J. M. (2014). Biocarbon monoliths as supercapacitor electrodes: Influence of wood anisotropy on their electrical and electrochemical properties. *Journal of The Electrochemical Society, 161*(12), A1806–A1811. https://doi.org/10.1149/2.0391412jes

Dai, W., Liu, Y., Wang, M., Lin, M., Lian, X., Luo, Y., ... Chen, W. (2021). Monodispersed ruthenium nanoparticles on nitrogen-doped reduced graphene oxide for an efficient lithium-oxygen battery. *ACS Applied Materials Interfaces, 13*(17), 19915–19926. https://doi.org/10.1021/acsami.0c23125

Deng, X., Jiang, Z., Chen, Y., Dang, D., Liu, Q., Wang, X., & Yang, X. (2023). Renewable wood-derived hierarchical porous, N-doped carbon sheet as a robust self-supporting cathodic electrode for zinc-air batteries. *Chinese Chemical Letters, 34*(1), 107389. https://doi.org/10.1016/j.cclet.2022.03.112

Dong, Z. H., Pan, X. H., Zhu, C., Tang, C. S., Lv, C., Liu, B., ... Shi, B. (2024). Bio-mediated geotechnology and its application in geoengineering: Mechanism, approach, and performance. *Environmental Earth Sciences, 83*(11), 348. https://doi.org/10.1007/s12665-024-11668-1.

Feng, J., Tang, R., Wang, X., & Wang, T. (2021). Biomass-derived activated carbon sheets with tunable oxygen functional groups and pore volume for high-performance oxygen reduction and Zn–Air batteries. *ACS Applied Energy Materials, 4*(5), 5230–5236. https://doi.org/10.1021/acsaem.1c00755

Gao, Y., Zhang, T., Mao, Y., Wang, J., & Sun, C. (2023). Highly efficient bifunctional layered triple Co, Fe, Ru hydroxides and oxides composite electrocatalysts for Zinc-Air batteries. *Journal of Electroanalytical Chemistry, 935, 117315*. https://doi.org/10.1016/j.jelechem.2023.117315

Ge, Z., Chen, X., Hao, X., Hu, S., Li, J., & Lai, H. (2023). Wood-derived density-adjustable hierarchical porous carbon frameworks for high-performance lithium-sulfur batteries. *Materials Letters, 331*, 133537. https://doi.org/10.1016/j.matlet.2022.133537

Goodenough, J. B., & Park, K. S. (2013). The Li-ion rechargeable battery: A perspective. *Journal of the American Chemical Society, 135*(4), 1167–1176. https://doi.org/10.1021/ja3091438

Guo, Z., Han, X., Zhang, C., He, S., Liu, K., Hu, J., ... Duan, G. (2024). Activation of biomass-derived porous carbon for supercapacitors: A review. *Chinese Chemical Letters, 35*(7), 109007. https://doi.org/10.1016/j.cclet.2023.109007

Huang, X., Huang, J., Yang, D., & Wu, P. (2021). A multi-scale structural engineering strategy for high-performance mxene hydrogel supercapacitor electrode. *Advanced Science, 8*(18), 2101664. https://doi.org/10.1002/advs.202101664

Huang, X., Sha, W., He, S., Zhao, L., Li, S., Lv, C., & Pan, H. (2023). Defect-rich Mo_2S_3 loaded wood-derived carbon acts as a spacer in lithium-sulfur batteries: Forming a polysulfide capture net and promoting fast lithium flux. *Nanoscale, 15*(17), 7870–7876. https://doi.org/10.1039/d3nr00580a

Huang, J., Zhao, B., Liu, T., Mou, J., Jiang, Z., Liu, J., ... Liu, M. (2019). Wood-derived materials for advanced electrochemical energy storage devices. *Advanced Functional Materials, 29*(31), https://doi.org/10.1002/adfm.201902255

Jain, A., Balasubramanian, R., & Srinivasan, M. P. (2016). Hydrothermal conversion of biomass waste to activated carbon with high porosity: A review. *Chemical Engineering Journal, 283*, 789–805. https://doi.org/10.1016/j.cej.2015.08.014

Jiang, J., He, P., Tong, S., Zheng, M., Lin, Z., Zhang, X., & Zhou, H (2016). Ruthenium functionalized graphene aerogels with hierarchical and three-dimensional porosity as a free-standing cathode for rechargeable lithium-oxygen batteries. *NPG Asia Materials, 8*(1), e239. https://doi.org/10.1038/am.2015.141

Jiang, Z. L., Sun, H., Shi, W. K., Cheng, J. Y., Hu, J. Y., Guo, H. L., ... Sun, S. G. (2019). P-doped hive-like carbon derived from pinecone biomass as efficient catalyst for Li–O2 battery. *ACS Sustainable Chemistry Engineering, 7*(16), 14161–14169. https://doi.org/10.1021/acssuschemeng.9b02790

Jin, C., Sheng, O., Lu, Y., Luo, J., Yuan, H., Zhang, W., ... Tao, X. (2018). Metal oxide nanoparticles induced step-edge nucleation of stable Li metal anode working under an ultrahigh current density of 15 mA cm^{-2}. *Nano Energy, 45*, 203–209. https://doi.org/10.1016/j.nanoen.2017.12.055

Jing, S., Gai, Z., Li, M., Tang, S., Ji, S., Liang, H., ... Tsiakaras, P. (2022). Enhanced electrochemical performance of a Li-O_2 battery using Co and N co-doped biochar cathode prepared in molten salt medium. *Electrochimica Acta, 410*, 140002. https://doi.org/10.1016/j.electacta.2022.140002

Jing, W., Wang, M., Li, Y., Li, H. R., Zhang, H., Hu, S., ... He, Y. B. (2021). Pore structure engineering of wood-derived hard carbon enables their high-capacity and cycle-stable sodium storage properties. *Electrochimica Acta, 391*, 139000. https://doi.org/10.1016/j.electacta.2021.139000

Johnson, L., Li, C., Liu, Z., Chen, Y., Freunberger, S. A., Ashok, P. C., ... Bruce, P. G. (2014). The role of LiO_2 solubility in O_2 reduction in aprotic solvents and its consequences for Li–O_2 batteries. *Nature Chemistry, 6*(12), 1091–1099. https://doi.org/10.1038/nchem.2101

Julien, C. M. (2023). Advanced materials for electrochemical energy storage: Lithium-ion, lithium-sulfur, lithium-air and sodium batteries. *International Journal of Molecular Sciences, 24*(3), 3026. https://doi.org/10.3390/ijms24033026

Jung, W. B., Park, H., Jang, J. S., Kim, D. Y., Kim, D. W., Lim, E., ... Jung, H. T. (2021). Polyelemental nanoparticles as catalysts for a Li-O_2 battery. *ACS Nano, 15*(3), 4235–4244. https://doi.org/10.1021/acsnano.0c06528

Kang, S., Li, X., Fan, J., & Chang, J. (2012). Characterization of hydrochars produced by hydrothermal carbonization of lignin, cellulose, d-xylose, and wood meal. *Industrial Engineering Chemistry Research, 51*(26), 9023–9031. https://doi.org/10.1021/ie300565d

Kim, S., Yang, H., Jeong, S., Lee, T., Chae, S., Lee, J. H., & Li, O. L. (2023b). Negative surface charge-mediated Fe Quantum dots with N-doped graphene/$Ti_3C_2T_x$ MXene as chlorine-resistance electrocatalysts for high performance seawater-based Al-air batteries. *Journal of Power Sources, 566*, 232923.

Kim, J. H., Kannan, A. G., Woo, H. S., Jin, D. G., Kim, W., Ryu, K., & Kim, D. W. (2015). A bi-functional metal-free catalyst composed of dual-doped graphene and mesoporous carbon for rechargeable lithium–oxygen batteries. *Journal of Materials Chemistry A, 3*(36), 18456–18465. https://doi.org/10.1039/c5ta05334j

Kim, K., Kim, J., & Moon, J. H. (2023a). The polysulfide-cathode binding energy landscape for lithium sulfide growth in lithium-sulfur batteries. *Advanced Science, 10*(12), Article e2206057.

Kopiec, D., Wrobel, P. S., Szeluga, U., & Kierzek, K. (2024). Facile method of preparation of carbon nanotubes based aerogels as cathodes for lithium-oxygen cells. *Journal of Power Sources, 604*, 234501. https://doi.org/10.1016/j.jpowsour.2024.234501

Li, Y., Fu, K. K., Chen, C., Luo, W., Gao, T., Xu, S., ... Hu, L. (2017). Enabling high-areal-capacity lithium–sulfur batteries: Designing anisotropic and low-tortuosity porous

architectures. *ACS Nano, 11*(5), 4801–4807. https://doi.org/10.1021/acsnano.7b01172

Li, X., Guan, Q., Zhuang, Z., Zhang, Y., Lin, Y., Wang, J., ... Ling, L. (2023). Ordered mesoporous carbon grafted MXene catalytic heterostructure as Li-Ion kinetic pump toward high-efficient sulfur/sulfide conversions for Li-S battery. *ACS Nano*. https://doi.org/10.1021/acsnano.2c11663

Li, D., Han, Z., Leng, K., Ma, S., Wang, Y., & Bai, J. (2021). Biomass wood-derived efficient Fe–N–C catalysts for oxygen reduction reaction. *Journal of Materials Science, 56*(22), 12764–12774. https://doi.org/10.1007/s10853-021-06122-7

Li, Y., Wang, X., Dong, S., Chen, X., & Cui, G. (2016). *Recent advances in non-aqueous electrolyte for rechargeable Li–O_2 batteries. Advanced Energy Materials, 6*(18), 1600751.

Li, Y., Xia, D., Tao, L., Xu, Z., Yu, D., Jin, Q., ... Huang, H. (2024). Hydrothermally assisted conversion of switchgrass into hard carbon as anode materials for sodium-ion batteries. *ACS Applied Materials & Interfaces, 16*(22), 28461–28472. https://doi.org/10.1021/acsami.4c02734

Liang, H., Gai, Z., Chen, F., Jing, S., Kan, W., Zhao, B., ... Tsiakaras, P. (2023). Fe_3C decorated wood-derived integral N-doped C cathode for rechargeable Li-O_2 batteries. *Applied Catalysis B Environmental, 324*, 122203. https://doi.org/10.1016/j.apcatb.2022.122203

Liu, Y., He, P., & Zhou, H. (2017). Rechargeable solid-state li–Air and Li–S batteries: Materials, construction, and challenges. *Advanced Energy Materials, 8*(4), https://doi.org/10.1002/aenm.201701602

Liu, Y. S., Ma, C., Bai, Y. L., & Wu, X. (2018). Nitrogen-doped carbon nanotube sponge with embedded Fe/Fe_3C nanoparticles as binder-free cathodes for high capacity lithium–sulfur batteries. *Journal of Materials Chemistry A, 6*(36), 17473–17480. https://doi.org/10.1039/c8ta06040a

Liu, J., Meng, X., Xie, J., Liu, B., Tang, B., Wang, R., & Zou, J. (2023). Dual active sites engineering on sea urchin-Like CoNiS hollow nanosphere for stabilizing oxygen electrocatalysis via a template-free vulcanization strategy. *Advanced Functional Materials, 33*(22), https://doi.org/10.1002/adfm.202300579

Liu, P., Wang, Y., & Liu, J. (2019). Biomass-derived porous carbon materials for advanced lithium sulfur batteries. *Journal of Energy Chemistry, 34*, 171–185. https://doi.org/10.1016/j.jechem.2018.10.005

Liu, J., Wang, L., Huang, Z., Fan, F., Jiao, L., & Li, F. (2022). Facile synthesis of high quality hard carbon anode from Eucalyptus wood for sodium-ion batteries. *Chemical Papers, 76*(12), 7465–7473. https://doi.org/10.1007/s11696-022-02397-5

Liu, L., Zhang, X., Yan, F., Geng, B., Zhu, C., & Chen, Y. (2020). Self-supported N-doped CNT arrays for flexible Zn–air batteries. *Journal of Materials Chemistry A, 8*(35), 18162–18172. https://doi.org/10.1039/d0ta05510g

Lou, R., & Wu, S. B (2011). Products properties from fast pyrolysis of enzymatic/mild acidolysis lignin. *Applied Energy, 88*(1), 316–322. https://doi.org/10.1016/j.apenergy.2010.06.028

Lu, J., Park, J. B., Sun, Y. K., Wu, F., & Amine, K. (2014). Aprotic and aqueous Li-O_2 batteries. *Chemical Reviews, 114*(11), 5611–5640. https://doi.org/10.1021/cr400573b

Luo, Y., Tang, Y., Bin, X., Xia, C., & Que, W. (2022). 3D porous compact 1D/2D Fe_2O_3/MXene composite aerogel film electrodes for all-solid-state supercapacitors. *Small, 18*(48), 2204917. https://doi.org/10.1002/smll.202204917

Luo, J., Yao, X., Yang, L., Han, Y., Chen, L., Geng, X., ... Zhu, H. (2017). *Free-standing porous carbon electrodes derived from wood for high-performance Li-O_2 battery applications. Nano Research, 10*(12), 4318–4326. https://doi.org/10.1007/s12274-017-1660-x

Lv, C., Liu, J., Guo, G., & Zhang, Y. (2022). The mechanical properties of plant fiber-reinforced geopolymers: A review. *Polymers, 14*(19), 4134. https://doi.org/10.3390/polym14194134

Lv, X. W., Wang, Z., Lai, Z., Liu, Y., Ma, T., Geng, J., & Yuan, Z. Y. (2024). Rechargeable zinc-air batteries: Advances, challenges, and prospects. *Small, 20*(4), Article e2306396. https://doi.org/10.1002/smll.202306396

Ma, L., Yu, T., Tzoganakis, E., Amine, K., Wu, T., Chen, Z., & Lu, J. (2018). *Fundamental understanding and material challenges in rechargeable nonaqueous Li–O_2 batteries: Recent progress and perspective. Advanced Energy Materials, 8*(22), 1800348. https://doi.org/10.1002/aenm.201800348

Marathe, S., & Sadowski, Ł. (2024). Developments in biochar incorporated geopolymers and alkali activated materials: A systematic literature review. *Journal of Cleaner Production,* 469. https://doi.org/10.1016/j.jclepro.2024.143136

Ming, J., Wu, Y., Liang, G., Park, J. B., Zhao, F., & Sun, Y. K. (2013). Sodium salt effect on hydrothermal carbonization of biomass: a catalyst for carbon-based nanostructured materials for lithium-ion battery applications. *Green Chemistry, 15*(10), 2722–2726. https://doi.org/10.1039/c3gc40480c

Nguyen, V. P., Park, J. S., Shim, H. C., Yuk, J. M., Kim, J. H., Kim, D., & Lee, S. M. (2023). Accelerated sulfur evolution reactions by TiS_2/TiO_2@MXene host for high-volumetric-energy-density lithium–sulfur batteries. *Advanced Functional Materials, 33*(35), https://doi.org/10.1002/adfm.202303503

Nomura, A., Ito, K., & Kubo, Y. (2017). CNT sheet air electrode for the development of ultra-high cell capacity in lithium-air batteries. *Scientific Reports, 7*(1), https://doi.org/10.1038/srep45596

Pang, H., Sun, P., Gong, H., Zhang, N., Cao, J., Zhang, R., ... Kong, B. (2021). Wood-derived bimetallic and heteroatomic hierarchically porous carbon aerogel for rechargeable flow Zn–Air batteries. *ACS Applied Materials Interfaces, 13*(33), 39458–39469. https://doi.org/10.1021/acsami.1c10925

Peng, X., Zhang, L., Chen, Z., Zhong, L., Zhao, D., Chi, X., ... Loh, K. P. (2019). Hierarchically porous carbon plates derived from wood as bifunctional ORR/OER electrodes. *Advanced Materials, 31*(16), 1900341. https://doi.org/10.1002/adma.201900341

Phiri, J., Dou, J., Vuorinen, T., Gane, P. A., & Maloney, T. C. (2019). Highly porous willow wood-derived activated carbon for high-performance supercapacitor electrodes. *ACS Omega, 4*(19), 18108–18117. https://doi.org/10.1021/acsomega.9b01977

Poudel, M. B., Balanay, M. P., Lohani, P. C., Sekar, K., & Yoo, D. J. (2024). Atomic engineering of 3D self-supported bifunctional oxygen electrodes for rechargeable zinc-air batteries and fuel cell applications. *Advanced Energy Materials, 14*(30), 2400347. https://doi.org/10.1002/aenm.202400347

Sabet, S. M., Sapkota, N., Chiluwal, S., Zheng, T., Clemons, C. M., Rao, A. M., & Pilla, S. (2023). Sulfurized polyacrylonitrile impregnated delignified wood-based 3D carbon framework for high-performance lithium–sulfur batteries. *ACS Sustainable Chemistry & Engineering, 11*(6), 2314–2323. https://doi.org/10.1021/acssuschemeng.2c05886

Schneidermann, C., Kensy, C., Otto, P., Oswald, S., Giebeler, L., Leistenschneider, D., ... Borchardt, L. (2019). Nitrogen-doped biomass-derived carbon formed by mechanochemical synthesis for lithium-sulfur batteries. *ChemSusChem, 12*(1), 310–319. https://doi.org/10.1002/cssc.201801997

Sevilla, M., & Fuertes, A. B. (2009). The production of carbon materials by hydrothermal carbonization of cellulose. *Carbon, 47*(9), 2281–2289. https://doi.org/10.1016/j.carbon.2009.04.026

Shan, X., Wu, J., Zhang, X., Wang, L., Yang, J., Chen, Z., ... Wang, X. (2021). Wood for application in electrochemical energy storage devices. *Cell Reports Physical Science, 2*(12), https://doi.org/10.1016/j.xcrp.2021.10065

Shu, C., Wang, J., Long, J., Liu, H. K., & Dou, S. X. (2019). Understanding the reaction chemistry during charging in aprotic lithium–oxygen batteries: existing problems and solutions. *Advanced Materials, 31*(15), 1804587. https://doi.org/10.1002/adma.201804587

Song, H., Chen, X., Zheng, G., Yu, X., Jiang, S., Cui, Z., ... Liao, S. (2019). Dendrite-free composite Li anode assisted by Ag nanoparticles in a wood-derived carbon frame. *ACS Applied Materials Interfaces, 11*(20), 18361–18367. https://doi.org/10.1021/acsami.9b01694

Song, S., Li, W., Deng, Y. P., Ruan, Y., Zhang, Y., Qin, X., & Chen, Z. (2020). TiC supported amorphous MnO_x as highly efficient bifunctional electrocatalyst for corrosion resistant oxygen electrode of Zn-air batteries. *Nano Energy, 67*, 104208. https://doi.org/10.1016/j.nanoen.2019.104208

Song, H., Xu, S., Li, Y., Dai, J., Gong, A., Zhu, M., ... Hu, L. (2017). Hierarchically porous, ultrathick, "breathable" wood-derived cathode for lithium-oxygen batteries. *Advanced Energy Materials, 8*(4), 1701203. https://doi.org/10.1002/aenm.201701203

Tan, C., Cao, D., Zheng, L., Shen, Y., Chen, L., & Chen, Y. (2022). True reaction sites on discharge in Li-O_2 batteries. *Journal of the American Chemical Society, 144*(2), 807–815. https://doi.org/10.1021/jacs.1c09916

Tang, Z., Zhang, R., Wang, H., Zhou, S., Pan, Z., Huang, Y., ... Shao, M. (2023). Revealing the closed pore formation of waste wood-derived hard carbon for advanced sodium-ion battery. *Nature Communications, 14*(1), 6024. https://doi.org/10.1038/s41467-023-39637-5

Tao, T., Lu, S., Fan, Y., Lei, W., Huang, S., & Chen, Y. (2017). Anode improvement in rechargeable lithium-sulfur batteries. *Advanced Materials, 29*(48), https://doi.org/10.1002/adma.201700542

Wang, H., Cui, Z., He, S. A., Zhu, J., Luo, W., Liu, Q., & Zou, R. (2022a). Construction of ultrathin layered MXene-TiN heterostructure enabling favorable catalytic ability for high-areal-capacity lithium–sulfur batteries. *Nano-Micro Letters, 14*(1), 189. https://doi.org/10.1007/s40820-022-00935-0

Wang, D., Dong, S., Ashour, A., Wang, X., Qiu, L., & Han, B. (2022b). Biomass-derived nanocellulose-modified cementitious composites: a review. *Materials Today Sustainability, 18*, 100115. https://doi.org/10.1016/j.mtsust.2022.100115

Wang, P., Guo, Y. J., Chen, W. P., Duan, H., Ye, H., Yao, H. R., ... Cao, F. F. (2022c). Self-supported hard carbon anode from fungus-treated basswood towards sodium-ion batteries. *Nano Research, 16*(3), 3832–3838. https://doi.org/10.1007/s12274-022-4708-5.

Wang, F., Chen, L., He, S., Zhang, Q., Liu, K., Han, X., ... Jiang, S. (2022d). Design of wood-derived anisotropic structural carbon electrode for high-performance supercapacitor. *Wood Science and Technology, 56*(4), 1191–1203. https://doi.org/10.1007/s00226-022-01389-8

Wang, Y., Wu, N., Qi, Y., Zhu, Z., Zhang, T., Han, X., ... Qiu, J. (2022e). Hollow iron carbides via nanoscale Kirkendall cavitation process for zinc-air batteries. *Applied Surface Science, 585*, 152569. https://doi.org/10.1016/j.apsusc.2022.152569

Wang, X., Du, D., Yan, Y., Ren, L., Xu, H., Wen, X., ... Shu, C. (2023a). Molecular cleavage strategy enabling optimized local electron structure of Co-based metal-organic framework to accelerate the kinetics of oxygen electrode reactions in lithium-oxygen battery. *Energy Storage Materials, 63*, 103033. https://doi.org/10.1016/j.ensm.2023.103033

Wang, F., Lee, J., Chen, L., Zhang, G., He, S., Han, J., ... Kim, I. D. (2023b). Inspired by wood: thick electrodes for supercapacitors. *ACS nano, 17*(10), 8866–8898. https://doi.org/10.1021/acsnano.3c01241

Wang, Y., Liu, Y., Zhou, L., Zhang, P., Wu, X., Liu, T., ... Li, B. (2023c). $Ni_3Fe/Ni_3Fe(OOH)_x$ dynamically coupled on wood-derived nitrogen doped carbon as a bifunctional electrocatalyst for rechargeable zinc–air batteries. *Journal of Materials Chemistry A, 11*(4), 1894–1905. https://doi.org/10.1039/D2TA09269G

Wang, W., Shen, L. L., Wu, P., Yu, H., Wang, J., Xu, Y., ... Mei, D. (2024). Transpiration-mimicking wood-based microfluidic aluminum-air batteries: Green power sources for miniaturized applications. *Chemical Engineering Journal, 480*. https://doi.org/10.1016/j.cej.2023.148104

Wen, Y., Shen, Z., Hui, J., Zhang, H., & Zhu, Q. (2023). Co/CoSe junctions enable efficient and durable electrocatalytic conversion of polysulfides for high-performance Li–S batteries. *Advanced Energy Materials, 13*(20), https://doi.org/10.1002/aenm.202204345

Wong, H., Liu, T., Tamtaji, M., Huang, X., Tang, T. W., Hossain, M. D., ... Luo, Z. (2024). Graphene-supported single atom catalysts for high performance lithium-oxygen batteries. *Nano Energy, 121*, 109279. https://doi.org/10.1016/j.nanoen.2024.109279

Wu, J., Dai, Q., Li, X., Li, W., Hao, S. M., Zeng, M. J., & Yu, Z. Z. (2021). Wood-derived monolithic ultrathick porous carbon electrodes filled with reduced graphene oxide for high-performance supercapacitors with ultrahigh areal capacitances. *ChemElectroChem, 8*(22), 4328–4336. https://doi.org/10.1002/celc.202100937.

Wu, F. C., Tseng, R. L., Hu, C. C., & Wang, C. C. (2004). Physical and electrochemical characterization of activated carbons prepared from firwoods for supercapacitors. *Journal of Power Sources, 138*(1–2), 351–359. https://doi.org/10.1016/j.jpowsour.2004.06.023

Wu, X., Yuan, X., Zhao, J., Ji, D., Guo, H., Yao, W., ... Zhang, L. (2023). Study on the effects of different pectinase/cellulase ratios and pretreatment times on the preparation of nanocellulose by ultrasound-assisted bio-enzyme heat treatment. *RSC Advances, 13*(8), 5149–5157. https://doi.org/10.1039/d2ra08172e.

Wu, C., Zhang, S., Wu, W., Xi, Z., Zhou, C., Wang, X., ... Chen, D. (2019). Carbon nanotubes grown on the inner wall of carbonized wood tracheids for high-performance supercapacitors. *Carbon, 150*, 311–318. https://doi.org/10.1016/j.carbon.2019.05.032

Xia, X., Zhan, J., Zhong, Y., Wang, X., Tu, J., & Fan, H. J. (2016). Single-crystalline, metallic TiC nanowires for highly robust and wide-temperature electrochemical energy storage. *Small, 13*(5), https://doi.org/10.1002/smll.201602742

Xing, Y., Chen, N., Luo, M., Sun, Y., Yang, Y., Qian, J., ... Wu, F. (2020). Long-life lithium-O_2 battery achieved by integrating quasi-solid electrolyte and highly active Pt_3Co nanowires catalyst. *Energy Storage Materials, 24*, 707–713. https://doi.org/10.1016/j.ensm.2019.06.008

Xu, J., Lei, J., Ming, N., Zhang, C., & Huo, K. (2022). Rational design of wood-structured thick electrode for electrochemical energy storage. *Advanced Functional Materials, 32*(35), https://doi.org/10.1002/adfm.202204426

Yan, Y., Liang, S., Wang, X., Zhang, M., Hao, S. M., Cui, X., ... Lin, Z. (2021). Robust wrinkled MoS_2/N-C bifunctional electrocatalysts interfaced with single Fe atoms for wearable zinc-air batteries. *Proceedings of the National Academy of Sciences of the United States of America, 118*(40), Article e2110036118. https://doi.org/10.1073/pnas.2110036118

Yan, B., Zhang, Q., Yang, G., He, C., Chen, J., Li, P., ... He, S. (2024). Improving the capacitive performance of wood-derived carbon monolith by anchoring heteroatom-doped carbon nanotubes in the vessels via in situ chemical vapor deposition. *Colloids and Surfaces A: Physicochemical and Engineering Aspects, 695*. https://doi.org/10.1016/j.colsurfa.2024.134263

Yang, Y., Li, N., Lv, T., Chen, Z., Liu, Y., Dong, K., ... Chen, T. (2022). Natural wood-derived free-standing films as efficient and stable separators for high-performance lithium ion batteries. *Nanoscale Advances, 4*(7), 1718–1726. https://doi.org/10.1039/d2na00097k

Yang, F., Yao, Y., Xu, Y., Wang, C., Wang, M., Ren, J., ... Lu, J. (2023). Evolution of the porous structure for phosphoric acid etching carbon as cathodes in Li–O_2 batteries: Pyrolysis temperature-induced characteristics changes. *Carbon Energy, 6*(1), https://doi.org/10.1002/cey2.372

Yao, B., Peng, H., Zhang, H., Kang, J., Zhu, C., Delgado, G., ... Li, Y. (2021). Printing porous carbon aerogels for low temperature supercapacitors. *Nano Letters, 21*(9), 3731–3737. https://doi.org/10.1021/acs.nanolett.0c04780

Yao, W., Yuan, Y., Tan, G., Liu, C., Cheng, M., Yurkiv, V., ... Shahbazian-Yassar, R. (2019). Tuning Li_2O_2 formation routes by facet engineering of MnO_2 cathode catalysts. *Journal of the American Chemical Society, 141*(32), 12832–12838. https://doi.org/10.1021/jacs.9b05992

Yao, W., Zheng, D., Li, Z., Wang, Y., Tan, H., & Zhang, Y. (2023). MXene@ carbonized wood monolithic electrode with hierarchical porous framework for high-performance supercapacitors. *Applied Surface Science, 638*, 158130. https://doi.org/10.1016/j.apsusc.2023.158130

Ye, L., Hong, Y., Liao, M., Wang, B., Wei, D., Peng, H., ... Peng, H. (2020). Recent advances in flexible fiber-shaped metal-air batteries. *Energy Storage Materials, 28*, 364–374.

Yu, W., Yoshii, T., Aziz, A., Tang, R., Pan, Z. Z., Inoue, K., ... Nishihara, H. (2023). Edge-site-free and topological-defect-rich carbon cathode for high-performance lithium-oxygen batteries. *Advanced Science, 10*(16), 2300268. https://doi.org/10.1002/advs.202300268

Yu, L., Shang, Z., Lin, X., Li, M., Liu, Y., Ren, L., ... Sun, X. (2024). Bio-derived wood-based gas diffusion electrode for high-performance aluminum–air batteries: Insights into Pore Structure. *Advanced Materials Interfaces, 11*(1), 2300355. https://doi.org/10.1002/admi.202300355

Yu, F., Li, S., Chen, W., Wu, T., & Peng, C. (2019). Biomass-derived materials for electrochemical energy storage and conversion: Overview and perspectives. *Energy Environmental Materials, 2*(1), 55–67. https://doi.org/10.1002/eem2.12030

Yuan, Z., Mao, H., Yu, D., & Chen, X. (2023a). Photo-assisted metal-air batteries: Recent progress, challenges and opportunities. *Chemistry–A European Journal, 29*(19), e202202920. https://doi.org/10.1002/chem.202202920

Yuan, M., Li, C., Liu, Y., Lan, H., Chen, Y., Liu, K., & Wang, L. (2023b). Single atom iron implanted polydopamine-modified hollow leaf-like N-doped carbon catalyst for improving oxygen reduction reaction and zinc-air batteries. *Journal of Colloid and Interface Science, 645*, 350–358. https://doi.org/10.1016/j.jcis.2023.04.162

Zeng, M. J., Li, X., Hao, S. M., Qu, J., Li, W., Wu, J., ... Yu, Z. Z. (2022a). Hierarchically porous graphene/wood-derived carbon activated using $ZnCl_2$ and decorated with in situ grown $NiCo_2O_4$ for high–performance asymmetric supercapacitors. *New Journal of Chemistry, 46*(2), 533–541. https://doi.org/10.1039/D1NJ05027C

Zeng, M. J., Li, X., Li, W., Zhao, T., Wu, J., Hao, S. M., & Yu, Z. Z. (2022b). Self-supported and hierarchically porous activated carbon nanotube/carbonized wood electrodes for high-performance solid-state supercapacitors. *Applied Surface Science, 598*, 153765. https://doi.org/10.1016/j.apsusc.2022.153765

Zhang, W., Xu, B., Zhang, L., Li, W., Li, S., Zhang, J., ... Du, L. (2022a). Co_4N-decorated 3D wood-derived carbon host enables enhanced cathodic electrocatalysis and homogeneous lithium deposition for lithium–sulfur full cells. *Small, 18*(6), 2105664. https://doi.org/10.1002/smll.202105664

Zhang, P., Liu, Y., Wang, S., Zhou, L., Liu, T., Sun, K., ... Li, B. (2022b). Wood-derived monolithic catalysts with the ability of activating water molecules for oxygen electrocatalysis. *Small, 18*(34), 2202725. https://doi.org/10.1002/smll.202202725

Zhang, L., Liu, Y., Liu, S., Zhou, L., Wu, X., Guo, X., ... Jiang, J. (2023a). Mn-doped Co nanoparticles on wood-derived monolithic carbon for rechargeable zinc–air batteries. *Journal of Materials Chemistry A, 11*(42), 22951–22959. https://doi.org/10.1039/D3TA05023H

Zhang, G., et al. (2023a). A multifunctional wood-derived separator towards the problems of semi-open system in lithium-oxygen batteries. *Advanced Functional Materials, 33*(40).

Zhang, P., Sun, K., Liu, Y., Zhou, B., Li, S., Zhou, J., ... Jiang, J. (2023b). Improving bifunctional catalytic activity of biochar via in-situ growth of nickel-iron hydroxide as cathodic catalyst for zinc-air batteries. *Biochar, 5*(1), 60. https://doi.org/10.1007/s42773-023-00259-1

Zhang, P., Liu, S., Zhou, J., Zhou, L., Li, B., Li, S., ... Jiang, J. (2024b). Co-adjusting d-band center of Fe to accelerate proton coupling for efficient oxygen electrocatalysis. *Small, 20*(20), 2307662. https://doi.org/10.1002/smll.202307662

Zhang, Y., Liu, Y., & Wu, X. (2024a). Easily prepared wood–derived hierarchically porous carbon for high–performance supercapacitors. *ChemistrySelect, 9*(16), e202304397. https://doi.org/10.1002/slct.202304397

Zhao, G., Liu, Y., Tang, L., Zhang, L., & Sun, K. (2019). Capacitive behavior based on the ultrafast mass transport in a self-supported lithium oxygen battery cathode. *ACS Applied Energy Materials, 2*(3), 2113–2121. https://doi.org/10.1021/acsaem.8b02154

Zheng, Y., Lu, Y., Qi, X., Wang, Y., Mu, L., Li, Y., ... Hu, Y. S. (2019). Superior electrochemical performance of sodium-ion full-cell using poplar wood derived hard carbon anode. *Energy Storage Materials, 18*, 269–279. https://doi.org/10.1016/j.ensm.2018.09.002

Zhong, L., Jiang, C., Zheng, M., Peng, X., Liu, T., Xi, S., & Lu, J. (2021). Wood carbon based single-atom catalyst for rechargeable Zn–Air batteries. *ACS Energy Letters, 6*(10), 3624–3633. https://doi.org/10.1021/acsenergylett.1c01678

Zhou, L., Li, J., Yin, J., Zhang, G., Zhang, P., Zhou, J., ... Sun, K. (2024). Heterostructure catalyst coupled wood-derived carbon and cobalt-iron alloy/oxide for reversible oxygen conversion. *Biochar, 6*(1), 54. https://doi.org/10.1007/s42773-024-00348-9

Zhou, B., Liu, Y., Wu, X., Liu, H., Liu, T., Wang, Y., ... Li, B. (2021). Wood-derived integrated air electrode with Co-N sites for rechargeable zinc-air batteries. *Nano Research, 15*(2), 1415–1423. https://doi.org/10.1007/s12274-021-3678-3

Zhou, B., Xu, N., Wu, L., Cai, D., Yu, E. H., & Qiao, J. (2024). Wood-derived freestanding integrated electrode with robust interface-coupling effect boosted bifunctionality for rechargeable zinc-air batteries. *Green Energy & Environment, 9*(12), 1835–1846. https://doi.org/10.1016/j.gee.2023.12.002.

Zhu, C., Du, L., Luo, J., Tang, H., Cui, Z., Song, H., & Liao, S (2018). A renewable wood-derived cathode for Li–O_2 batteries. *Journal of Materials Chemistry A, 6*(29), 14291–14298. https://doi.org/10.1039/c8ta04703k

Zhu, H., Luo, W., Ciesielski, P. N., Fang, Z., Zhu, J. Y., Henriksson, G., ... Hu, L. (2016). Wood-derived materials for green electronics, biological devices, and energy applications. *Chemical Reviews, 116*(16), 9305–9374. https://doi.org/10.1021/acs.chemrev.6b00225